CHAPTER V

APPLICATIONS

(...) «Hay un lugar y uno solo al que de veras pertenecemos, un lugar que a menudo no es aquél donde nacimos, un lugar que se parece al paraíso. (...) Para crear una nueva sociedad, para dar comienzo a cualquier proyecto que valga la pena, uno debe dejar el lugar de su nacimiento. No podemos crecer si no rompemos ese lazo que nos ata al pasado, si no aprendemos a abrirnos a lo que es extraño y foráneo y fértil.» (pp. 372 -373)

ARIEL DORFMAN (from "Heading South, Looking North")

5.1. INTRODUCTION

CLOG has been applied to some synthetic cases. One of such cases was the "calcite example", which consisted of a confined limestone aquifer where water that was more acid than groundwater was recharged throughout the whole thickness of the formation. The example was interesting to study the influence of two clogging processes (attachment of suspended particles carried by recharge water and dissolution of the carbonaceous matrix). A description of the "calcite example" can be found in PÉREZ-PARICIO & CARRERA (1998a).

However, the aim of this work is to show the results of applications of the model to real datasets and real clogging problems. This chapter includes four different simulations, three of them corresponding to laboratory data and the fourth one to field data (Table 5.1.):

1. Laboratory examples.
   - Clogging by suspended particles in a radial sector (acronym KWAD). Data were collected by the Centre for Groundwater Studies [CGS], Adelaide, Australia. Potable water was injected in the apex of a 90º sector reproducing the conditions of radial flow. The aquifer material was composed of sand. Variables such as the concentration of solids, initial transmissivity and configuration of the well (with and without gravel-pack) were modified to measure their influence on piezometric heads (OSEI-BONSU, 1996).
   - Clogging by bacterial growth in a sand column (acronym DANE). Data were collected in the Technical University of Denmark [DTU]. The experiments consisted in injecting untreated lake water through sand columns in order to mimic open reservoir infiltration (ALBRECHTSEN ET AL., 1998; 1999). Bacterial clogging accounted for the significant reduction observed in hydraulic conductivity.
   - Clogging by suspended particles and bacterial growth together with chemical unclogging in calcite columns recharged with tertiary effluent (acronym STEPH). Data were obtained in a collaborative research among several Australian and French organisations. The objective was to gain insight into the expectable clogging and redox reactions at the field scale (RINK-PFEIFFER ET AL., 1998; 2000).

Table 5.1. Data of the examples presented in Chapter V. All of them consist of transient flow and transport problems with different clogging processes incorporated.

CASE	FLOW PATTERN	REAL[b] GEOMETRY	HYDRAULIC COND[c]	AQUIFER[d]	FLOWRATE & INF. RATE	TRANSPORT PROPERTIES	RECHARGE WATER	CLOGGING PROCESSES[e]	CLOG SPECIES[f]	CLOG MINERALS
LANG	Radial 2-D Horizontal domain	X=20 m Y=10 m	25 m/d	Fine sands C_u=1.0 (n.a.) $d_g=250\cdot10^{-6}$ m	Q=840 $m^3\cdot d^{-1}$ i= 22.3 $m\cdot d^{-1}$	ϕ=0.10 α=1.00 m D_m=0 m^2/d	Groundwater +Fe coag.ul. +aeration+RSF $d_p=25\cdot10^{-6}$ m	- Particles	Particles, H^+ OH^-	-Particles
KWAD[a]	Radial 2-D Vertical section	R=1.30 m Z=0.01 m	A) Aquifer: 20 m/d	Fine sands C_u=4.3 $d_g=250\cdot10^{-6}$ m	Q=2 $L\cdot min^{-1}$ i=73.3 $m\cdot d^{-1}$	ϕ=0.20 α=0.50 m D_m=0 m^2/d	Tap water $d_p=70\cdot10^{-6}$ m	-Particles: CF	Particles, H^+ OH^-	-Particles
			B) Gravel-pack: 400 m/d	Coarse sands C_u=2.0 $d_g=2220\cdot10^{-6}$ m	Q=2 $L\cdot min^{-1}$ i=73.3 $m\cdot d^{-1}$		Tap water $d_p=28\cdot10^{-6}$ m	-Particles: DBF-CF		
			C) Gravel-pack: 10÷400 m/d	Coarse sands C_u=1.4 $d_g=650\cdot10^{-6}$ m	Q=10 $L\cdot min^{-1}$ i=366.7 $m\cdot d^{-1}$		Tap water $d_p=28\cdot10^{-6}$ m	-Particles: DBF		
DANE	Vertical 1-D	Z=0.25 m Δ=0.10 m	4.3 m/d	Fine sands C_u=1.0 (n.a.)	Q=1.26 $L\cdot h^{-1}$ i=0.96 $m\cdot d^{-1}$	ϕ=0.15 α=0.10 m D_m=0 m^2/d	Unfiltered lake water	-Bacteria	CH_2O, $O_{2(aq)}$, H^+ OH^-	-Aerobic bacteria
STEPH	Vertical 1-D	Z=0.16 m Δ=0.05 m	0.70 m/d	Limestone C_u=60.0 $d_g=8\cdot10^{-6}$ m	Q=208 $mL\cdot h^{-1}$ i=10.2 $m\cdot d^{-1}$	ϕ=0.15 α=0.10 m D_m=0 m^2/d	Treated wastewater (secondary + DAF/F) $d_p=0.5\cdot10^{-6}$ m	-Particles -Bacteria -Calcite dissolution	Particles, H^+, Ca^{+2}, CH_2O, $O_{2(aq)}$, NO_3^-, NO_2^-, HCO_3^- OH^-, $CO_{2(aq)}$, CO_3^{-2}	-Particles -Bacteria: -Aerobic -Nitrobacter -Denitrifying -Calcite

[a]Three experiments were conducted, each with different grain size distributions of the aquifer material. A series consisted of a homogeneous aquifer without gravel-pack; the others (B and C series), with gravel-pack. Initial aquifer hydraulic conductivity was 20 m/d, whilst the permeability of the gravel-pack varied as a consequence of clogging.

[b]R means radial direction; X is distance along x-axis; Y is distance along y-axis; Z is distance along vertical (gravity) axis; Δ is the diameter of the column, which is indicated here because it has to be used to translate flowrates into infiltration rate values.

[c]Intrinsic permeability values and transmissivity values have been converted into hydraulic conductivity values for the sake of uniformity. In KWAD, the first K value is valid for all the three series, since it refers to the aquifer. The other two values apply to the conductivity of the gravel-pack (note that it varies very much in series C).

[d]The uniformity coefficient of the aquifer grains, C_u, is based on the grain size distribution. It is defined as $C_u=d_{60}/d_{10}$, i.e. the ratio of the sizes that 60 % and 10 %, respectively, of the particles (expressed by weight) can pass in a classical sieving analysis.

[e]CF means cake-filtration and DBF refers to deep-bed-filtration.

[f]Mobile species are split up into primary species (upper group) and secondary species (lower group).

2. Field applications.
   Only the Langerak case (acronym LANG) has been included because it is hard to obtain accurately documented measurements of real field experiments. This example shows how low concentrations of small iron flocs may lead to significant clogging problems during recharging fine-grained aquifers through wells (TIMMER & STUYFZAND, 1998; TIMMER ET AL., 1999).

The description of each example follows the same pattern. First, an introduction about the experiment objectives and characteristics is given. Second, the experimental setup is described. Third, the modelling approach, including both the conceptual and numerical assumptions, is presented. Fourth, the results of the model are briefly discussed. A synthesis of the more important findings is postponed to Chapter 6 in order to achieve a more compact and consistent document.

The STEPH case is presented in the last term because it comprises three clogging processes, which makes it more interesting. In order not to mix the rest of laboratory cases with the LANG case, this is described first.

5.2. IRON FLOCS IN RECHARGE WELLS (Langerak, the Netherlands)

5.2.1. INTRODUCTION TO *LANG*

Well recharge for urban water supply has been used for years on a test scale in the dune area of the Netherlands, but it was not applied in the polder area in the west of the country. Well recharge is viewed to combine the advantages surface water and groundwater, so that one of the water companies of the province of South Holland (*Watermaatschappij Zuid-Holland Oost*, WZHO) started the first field tests in 1994 (TIMMER & STUYFZAND, 1998). The potential sources for recharge were identified, and it was found that intensively treated river Rhine water would be adequate in terms of quality, guarantee of supply and cost. Treated Rhine water was produced by the company *NV Watertransportmaatschappij Rijn-Kennemerland* (WRK), in Nieuwegein. The recharge site was located in Langerak, at some 20 km Southwest of the production plant. The site consists of fine sand layers that are confined by clayey materials.

The goal of the Langerak test was to gain insight into the causes and cures of well clogging, and the changes in water quality during aquifer passage. This information was needed to design a full-size well recharge system and to design the post-treatment plant for water recovered from the aquifer. Unfortunately, the pipeline connecting Langerak with the WRK plant was not operative. This is why two tests were simultaneously carried out, one in Langerak (with native groundwater) and the other one in Nieuwegein (with water from WRK). The experimental design aimed at an identical recharge situation for both locations. In fact, all the major components of the recharge scheme (hydrogeology, recharge water quality, drilling method, recharge speed, etc) were identical in both sites. Recharge water in Langerak was produced from local groundwater by aeration and rapid sand filtration; in order to make its oxidation capacity comparable with that of WRK water, sodium nitrate ($NaNO_3$) was continuously added to it.

The Langerak site (the Netherlands) has been subjected to exhaustive investigations, whose results can be found in TIMMER & STUYFZAND (1998). Studies have focused on hydrochemistry of the site and the impact of Artificial Recharge on groundwater quality evolution. Complex hydrochemical modelling has also been performed during the EU Project in order to learn lessons from real sites where there exists comprehensive measured data (BRUN ET AL., 1998; SAALTINK ET AL., 1998b; SAALTINK, 1999).

5.2.2. EXPERIMENTAL SET-UP OF *LANG*

The test field consisted of two wells, an injection and recovery well, distanced by 190 m. Oxidised water was continuously injected (35 $m3 \cdot h^{-1}$, or 9.7 $L \cdot s^{-1}$) for over one year into a sandy aquifer that initially contained good-quality reduced water. Simultaneously, the recovery well pumped out water at the same rate. This produced the well-known dipole pattern. The recharge well had a diameter of 0.30 m. A gravel-pack was installed between a radius of 0.15 and 0.50 m. The 40-m thick aquifer was formed by fine sands, with an estimated transmissivity of 1,000 $m^2 \cdot d^{-1}$.

Recharge water had a good quality, as it was produced from native groundwater. For instance, recharge water had average concentrations of 91.5 $mg \cdot L^{-1}$ chloride, 60 $mg \cdot L^{-1}$ calcium and 8 $mg \cdot L^{-1}$ oxygen. In spite of the numerous preventive measures, the recharge well experienced a serious piezometric head build-up after 10 months of continuous injection of treated native groundwater. Recharge began in July, 1996, but it was not until May, 1997 that clogging effects were slightly observable. In summer 1997, there was a sudden head build-up (around 3.3 m in 4 months with

respect to the steady state previous condition) at the recharge borehole, indicating a severe clogging. Operation stopped in mid-September 1997 in order to restore the well capacity. After an efficient redevelopment, clogging rapidly occurred once again. Thanks to some pumping interruptions, recharge could be maintained up to April 1998, but results demonstrate the importance of clogging.

According to TIMMER & STUYFZAND (1998), clogging was most likely caused by residual iron particles, $Fe(OH)_3$, carried by drinking water from the local treatment plant. Iron flocs were generated during preparation of recharge water, which consisted of aeration and rapid sand filtration of local groundwater with significant concentration of dissolved (ferrous) iron. The concentration of iron flocs in recharge water was only 40 μg/l, whilst the size of particles ranged between 15 and 40 μm. By controlling the head evolution in the recharge well itself, in the gravel-pack and in the aquifer formation, Timmer & Stuyfzand (1998) concluded clogging took place almost entirely at the interface between the gravel-pack and the formation. Examples of this phenomenon are frequent in the literature (Bichara, 1986; Osei-Bonsu, 1996; Pérez-Paricio, 1998).

On contrary, the recharge well located in Nieuwegein did not clog. Apparently, the whole pre-treatment process was enough to prevent clogging. Activated carbon filtration was very efficient at removing undesired compounds from recharge water. The rest of section 5.2. is devoted to describing the numerical model of LANG.

5.2.3. MODELLING *LANG*

Modelling Langerak in terms of clogging was done within the framework of the European Union Project "Artificial Recharge of Groundwater", which was operative between 1996 and 1999. The modelling process comprised three steps. In all cases a 2-D horizontal medium was taken. In theory, it would have been enough with a 1-D medium, because clogging generally affects an aquifer volume that is located in the vicinity of the recharge well and it is possible to take advantage of radial symmetry. In addition, it was interesting to study conceptually the effect of small heterogeneities on the behaviour of the system.

The 3-step simulation consisted of the following work:

Step 1: Execution of simulations with an *extended* mesh to obtain the boundary conditions for a *detailed model* which had to be used in the final stage. A homogeneous transmissivity (1,000 $m^2 \cdot d^{-1}$) was used for the whole domain, which consisted of triangular finite elements in a 5,000x5,000 m mesh. The simulated domain was so large to avoid artificial boundary effects on the final piezometric head distribution. Due to symmetry (dipole flow pattern), only one quarter of the domain was considered. Symmetry enabled to impose a constant head condition at the right boundary, whilst the lower one had a no flow condition. The remaining boundaries had a mixed condition. Piezometric heads were computed in steady state, because data from Langerak suggest that equilibrium is reached very rapidly when recharge commences. The TRANSIN-II code (MEDINA ET AL. 1995), for inverse calibration of flow and transport, was utilised.

Step 2: When clogging occurs it generally affects an aquifer volume that is located in the vicinity of the recharge well. Therefore, it is not important to extend the analysis to a large aquifer portion. This is also the case in Langerak, as reported by Timmer & Stuyfzand (1998). By controlling the head evolution in the recharge well itself, in the gravel-pack and in the aquifer formation, they concluded that in Langerak clogging takes place almost entirely at the interface between the gravel-pack and the formation. Examples of this phenomenon are numerous (Bichara, 1986; Osei-Bonsu, 1996; Pérez-Paricio, 1998). A 20x10 m *detailed model* was built based on the heads obtained in the previous step (Figure 5.1.). The 0.15 m radius well was explicitly considered,

along with the gravel-pack (from 0.15 m up to 0.50 m in radial direction). Except for the lower boundary, which had a no-flow condition, prescribed heads as obtained from step 1 were fixed at all the boundaries. Table 5.2. collects the essential geometric and flow properties of both models.

Step 3: The *detailed* model was used to perform clogging computations (*clogging* model). The model analysed the transport of large particles within the aquifer and their impact on groundwater heads, but it did not include chemical reactions because they were not recognised to affect the hydraulic conductivity of the medium.

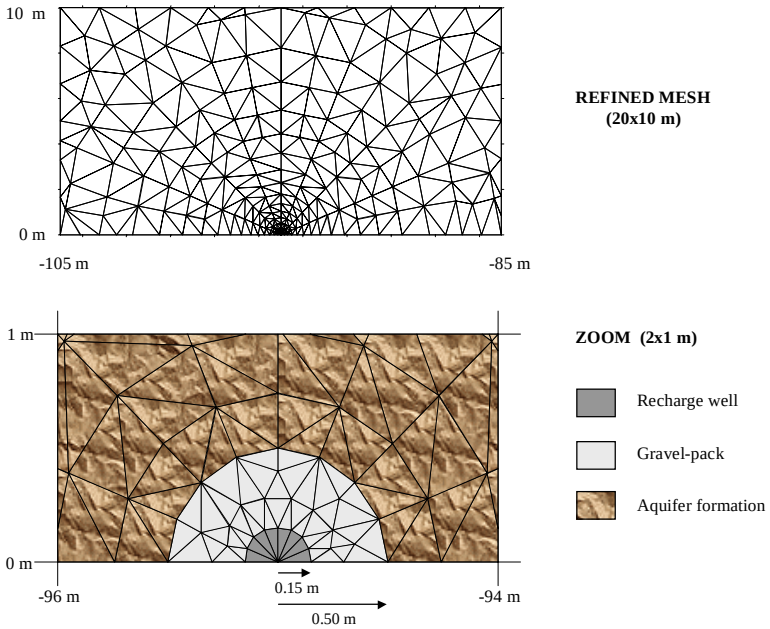

Figure 5.1. Finite element mesh corresponding to the *detailed model* simulation (left), size 20x10 m.
A zoom of this mesh in the immediate vicinity of recharge well is shown too (below), size 2x1 m. It is possible to distinguish the recharge well, the gravel-pack and the aquifer formation.

Table 5.2. Adopted conditions for the *extended* and the *detailed* models.
Both accounted for dipole flow symmetry, so that the simulated domain was just one quarter of the real problem.

		***EXTENDED* MODEL**	***DETAILED* MODEL**
Boundary	Left boundary	Cauchy	Dirichlet
	Upper boundary	Cauchy	Dirichlet
	Right boundary	Cauchy	Dirichlet
	Lower boundary	Cauchy	Neuman (no flow)
Geometry	2-D domain size [m]	5,000x5,000	20x10
	Number of nodes / elements	4969 / 9681	234 / 406
	Well	Point source	8 elements
	Gravel-pack	Not considered	42 elements
Model Parameters	Pumping rate [m^3/h]	35	35
	Aquifer transmissivity [$m^2 \cdot d^{-1}$] / grain size [m]	1,000 / -	1,000 / 0.001
	Gravel-pack transmissivity [$m^2 \cdot d^{-1}$] / grain size [m]	10,000 / -	10,000 / 0.01
	Transmissivity of heterogeneities* [$m^2 \cdot d^{-1}$]	-	500 – 10,000

*Values of the negative and positive (lower and higher, respectively, than the aquifer transmissivity) heterogeneities that are discussed in section 5.2.4.

5.2.4. *LANG* RESULTS

Figure 5.2. shows the calibration results for the recharge well and the aquifer. Calibration was satisfactory both in terms of temporal and spatial evolution. However, model results had a tendency to overestimate the extent of clogging in the first part of the response, thereby smoothing the shape of the curve. An explanation for this effect is the oversimplification of the conceptual model, because ideal boundary conditions and homogeneous hydraulic conductivity had to be assumed due to the lack of additional information. The difference between the initial and the final porosity at each node is also depicted in Figure 5.2. From both graphs, it is evident that clogging concentrated at the interface between the gravel-pack and the aquifer, in accordance with the experimental observation.

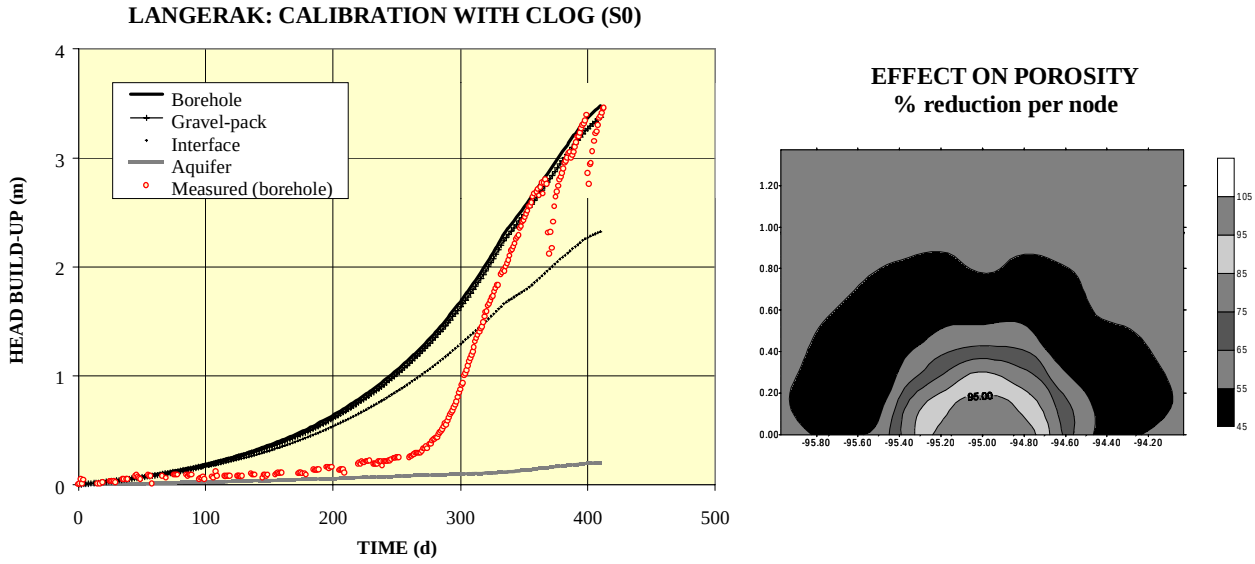

Figure 5.2. Calibration of measured data with CLOG.
On the left, the calibration of the calculated with respect to the measured piezometric head in the recharge well is shown for the 410 days period. On the right, an approximation is given to the ratio of the final porosity to the initial porosity in %, per each node, (zoom of ca. 1 m around the well). The right picture clearly demonstrates that clogging concentrated at the interface between the gravel-pack and the aquifer formation. Please note that porosity did not increase at any point; the value 105 in Figure 2b is only caused by the drawing interval.

A remark has to be done concerning these results. In a previous work, PÉREZ-PARICIO & CARRERA (1999e) showed a much better calibration that produced a close agreement between computed and measured values. But such calibration was achieved with a model that included two additional parameters, whose physical meaning could be unclear. In that work, it was conjectured that both extra parameters would account for cake filtration without and with compression (SCHIPPERS & VERDOUW 1980). With the inclusion of such parameters, it was possible to reproduce accurately the sharp head build-up experienced in the recharge well. On the grounds of producing a sound model, though, it has been considered more important to focus on the physics of the problem rather than providing exact fits. This is why in the remaining of section 5.2.4. only the results obtained with the simple parameterisation will be discussed.

Kinetic model parameters corresponding to this simplified model are shown in Table 5.3. Kinetic parameters (Chapter III) include the following:

- attachment and detachment constants, λ'_{att} and λ'_{det},
- interception exponent, m_{int}, whose value is comprised between 1.0 and 2.0
- compressibility of the particles, β_s, which is assumed to be higher than 1.0

- critical porosity ratio, ϕ/ϕ_{crit}.

There are other parameters that must be supplied to the numerical model, but they can be inferred from direct measurements or estimates. Consequently, those values can not be considered strictly as parameters, and, in fact, are assumed to be fixed. This is the case of the density (2,300 kg·m-3) and size ($30 \cdot 10^{-6}$ m) of the suspended particles, and the mean diameter of the aquifer grains in the gravel-pack ($10 \cdot 10^{-4}$ m) and aquifer ($1 \cdot 10^{-4}$ m). The transmissivities in these two zones were 10,000 and 1,000 $m^2 \cdot d^{-1}$, respectively. Porosity was set at 0.10 for the aquifer, 0.15 for the transition zone between gravel-pack and formation, and 0.20 in the gravel-pack.

Table 5.3. Model kinetic parameters for Langerak.
Column S0 contains the values of the parameters (optimum configuration) that led to the best agreement between computations and measurements. The rest of simulations (S1 through S8) constitute the sensitivity analysis. In each of the sensitivity runs, only one of the parameters was changed (dark background). Simulation S1 (S2) represents a 50 % decrease (increase) with respect to the optimum value, respectively. The same is valid for simulations S3 and S4 in relation with the detachment constant; S5 and S6, for the critical porosity ratio; S7 and S8, for the compressibility of the sediments. Only one simulation (increasing the parameter by a 50 %) was done for the interception exponent, given that its value must range between 1.0 and 2.0 (Chapter III).

		Calibration	**Sensitivity analysis**								
PARAMETER	**SYMBOL**	**S0**	**S1**	**S2**	**S3**	**S4**	**S5**	**S6**	**S7**	**S8**	**S8**
Attachment constant	λ'_{att} [$m \cdot s^{-1}$] * 10^{-4}	1.0	0.5	1.5	1.0	1.0	1.0	1.0	1.0	1.0	1.0
Detachment constant	λ'_{det} [s^{-1}] *10^{-8}	6.0	6.0	6.0	3.0	9.0	6.0	6.0	6.0	6.0	6.0
Critical porosity ratio	ϕ/ϕ_{crit} [-]	0.5	0.5	0.5	0.5	0.5	0.25	0.75	0.5	0.5	0.5
Compressibility of retained particles	β_s [-]	30.0	30.0	30.0	30.0	30.0	30.0	30.0	15.0	45.0	30.0
Interception exponent	m_{int} [-]	1.0	1.0	1.0	1.0	1.0	1.0	1.0	1.0	1.0	1.5

Several runs with modifications of the optimum configuration (S0) were conducted with the purpose of assessing the sensitivity of the model results to the model parameters. The procedure consisted in taking the values of simulation S0 (optimum configuration); then, each parameter was reduced (S1, S3, ...) or increased (S2, S4, ...) by a 50 % while the rest of parameters was fixed (Figure 5.3.).

It was found that the sensitivity of the model to the compressibility of the particles was significant (simulations S7 and S8). The attachment constant was the second most influential parameter based on the response to the new value (simulations S1 and S2). On contrary, the detachment constant (simulations S3 and S4) and the critical porosity value (simulations S5 and S6) were not very influential. The interception exponent also played a sensible role in heads build-up (S9), but this is not crucial because a constant value of 1.0 was adopted in all simulations.

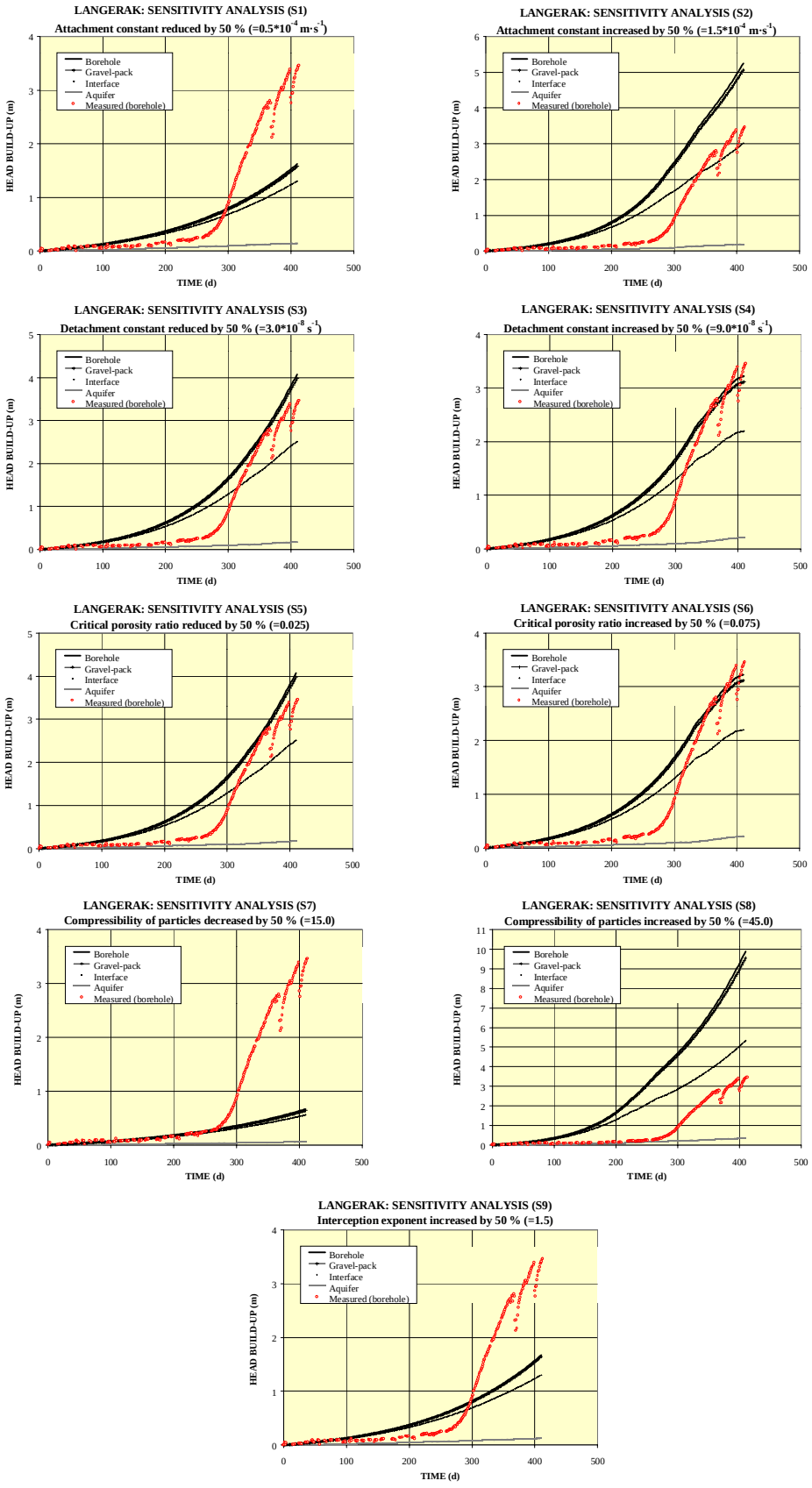

Figure 5.3. Sensitivity analysis to the model parameters for the Langerak case.
Only one parameter changed in each simulation with respect to the optimum configuration (**S0**).
S1-S2: λ'_{att} reduced/increased by 50 % (optimum value: 10^{-4} m·s^{-1}). **S3-S4**: λ'_{det} reduced/increased by 50 % (optimum: $6.0 \cdot 10^{-8}$ s^{-1}). **S5-S6**: ϕ/ϕ_{crit} 50 % lower and higher (optimum: 0.050). **S7-S8**: β_s 50 % lower/higher (optimum: 30.0). **S9**: m_{int} augmented by 50 % (optimum: 1.5). Notice that the scale of the vertical axis is not fixed.

A last simulation was carried out to compare the calibrated situation with a hypothetical case where a more conductive portion of the aquifer existed in the contact between the gravel-pack and the aquifer grains (Figure 5.4.). This patch was generated by modifying the effective porosity and transmissivity in a small region of the aquifer that was close to the interface. The modified values are compared to the original values in Table 5.4.

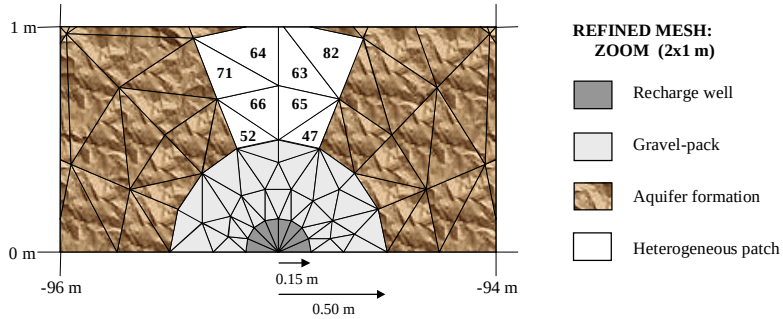

Figure 5.4. Picture of the heterogeneous patch artificially introduced to the model.
The patch was inserted in the contact of the aquifer with the gravel-pack in order to analyse the influence of positive (more conductive) and negative (less conductive) heterogeneities. Figures within the heterogeneity indicate the numbering of the elements included in the patch.

Table 5.4. Values assigned to the porosity and transmissivity of the heterogeneous patch.
Two situations were considered: positive heterogeneity (patch more conductive than the original) and negative heterogeneity (less conductive).

	Transmissivity [$m^2 \cdot d^{-1}$]	**Grain size diameter [m]**	**Porosity [-]**
Aquifer	1,000	$250 \cdot 10^{-6}$	0.10
Gravel-pack	10,000	$1{,}000 \cdot 10^{-6}$	0.20
Interface	1,000	$250 \cdot 10^{-6}$	0.15
Positive heterogeneity (K>)	10,000	$250 \cdot 10^{-6}$	0.15
Negative heterogeneity (K<)	100	$250 \cdot 10^{-6}$	0.05

Figure 5.5. shows the response of piezometric head in the recharge well (borehole) for both situations. The effect on porosity is also plotted in terms of percentage of reduction. It is evident that even small heterogeneities can play a crucial role on the evolution of recharge wells. In this simulation, the existence of the conductive path (positive heterogeneity) had a beneficial influence on clogging velocity. The negative heterogeneity led to a completely different response. However, it is quite remarkable that, if a longer simulation period is allowed, the piezometric build-up can be as significant as in the standard situation. Therefore, as far as concerns clogging, heterogeneities will control the velocity of efficiency reduction in the recharge system. This justifies the adoption of restrictive preventive measures even in high permeable formations in order to impose a limitation on heads build-up (PÉREZ-PARICIO & CARRERA, 1999a).

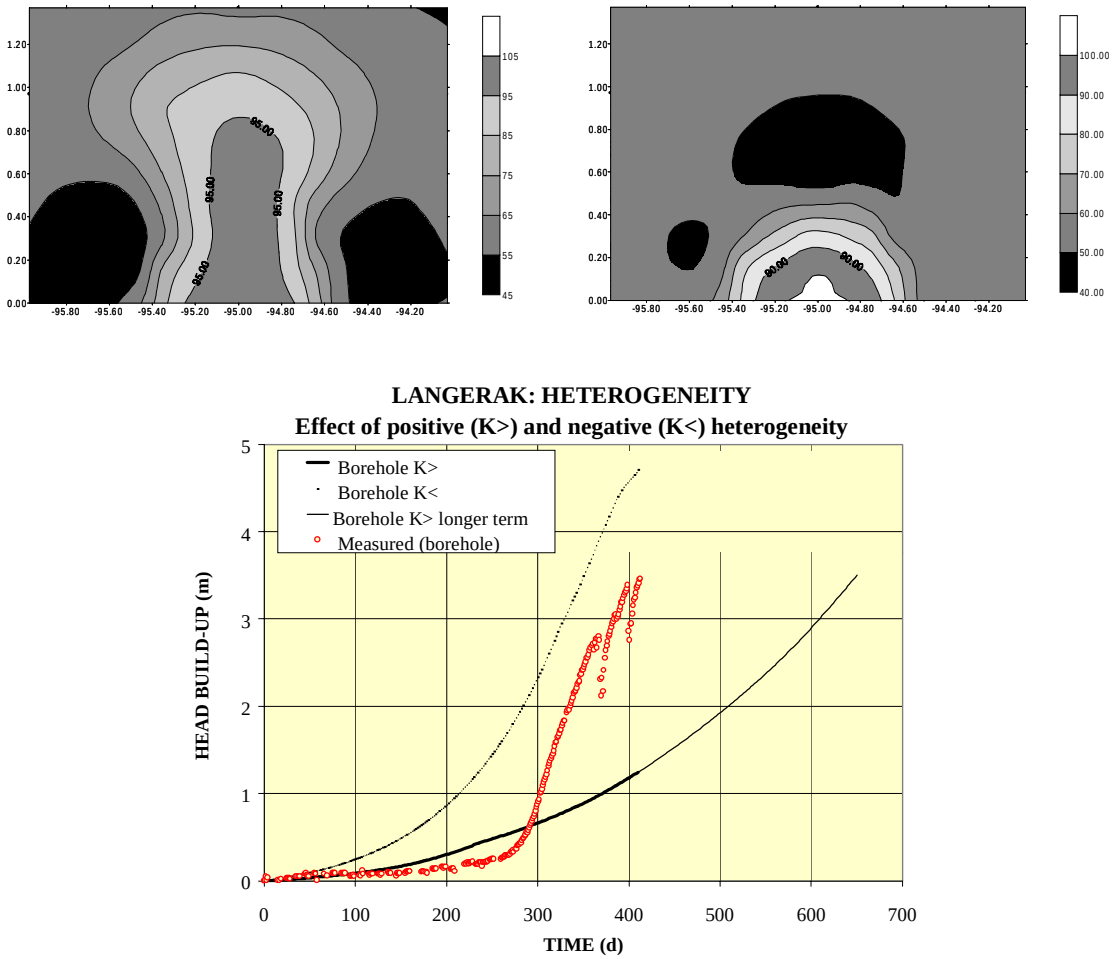

Figure 5.5. Effect of a small heterogeneity on the clogging impact.

(Above): on the left, the existence of a more permeable patch induces a preferential direction that is not clogged in comparison with the real situation (S0). The right picture presents the clogging pattern when a less permeable patch exists. Notice that the porosity is lower than in the real case, although the large-scale intervals do not permit a more accurate distinction.

(Below): comparison of the piezometric head for the real situation (measured) and the positive (K>) and negative (K<) heterogeneities. The values of transmissivity in the heterogeneous patch were 10,000 $m^2 \cdot d^{-1}$ (K>) and 100 $m^2 \cdot d^{-1}$ (K<), whilst the simulation value was 1,000 $m^2 \cdot d^{-1}$. A last simulation (650 days instead of 410) was done to assess the effect of longer recharge period for the positive heterogeneity. It was found (K> longer term) that the final build-up is comparable to the one obtained in the field.

5.3. SEDIMENTS IN A RADIAL SECTOR (Adelaide, South Australia)

5.3.1. INTRODUCTION TO *KWAD*

Clogging by suspended sediments carried by the injection fluid is one of the primary concerns associated with Artificial Recharge through wells. In spite of this, there is no much work on well recharge under radial-flow conditions. BICHARA (1986) carried out different tests on a 45^0 segment of an aquifer to investigate the effect of grain size distribution and concentration of suspended solids, filter-pack thickness and entrance velocities. Results indicated that the amount of suspended solids required to clog a gravel-packed well is 10 to 15 times the amount needed to plug a similar non filter-packed well. In the former case head losses occurred mainly at the filter-pack/aquifer interface, whilst sediments deposited on the surface of the aquifer (borehole) for non-filtered wells. Additional investigations on redevelopment techniques (BICHARA, 1988) led to the conclusion that gravel-packed wells are more difficult to redevelop than non gravel-packed ones.

OSEI-BONSU (1996) conducted similar experiments on a 90^0 segment of confined aquifer to assess the influence of the concentration and size of suspended solids and the configuration of the well (with and without gravel-pack) on clogging. He also proposed an analytical model to account for the two distinct observed mechanisms: blocking filtration, which took place for the non-filter well, and deep bed filtration, which occurred for the gravel-packed well.

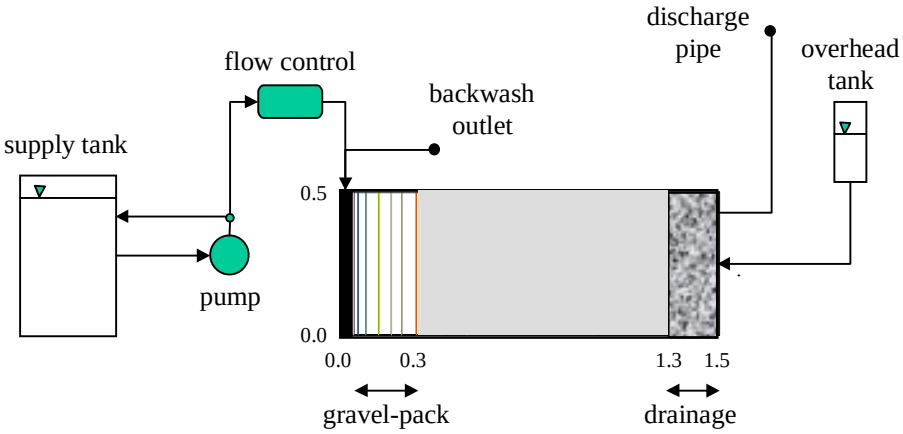

Figure 5.6. Diagram of the experimental apparatus of KWAD example.
The scheme displays the major components of the system: flow control device, redevelopment unit, injection water deposit and suspended solids tank, and the physical model with an indication on the distribution of the piezometers (from OSEI-BONSU, 1996). Twelve piezometers were installed along the central axis of the model.

5.3.2. EXPERIMENTAL SET-UP OF *KWAD*

A complete description of the experimental set-up is available in OSEI-BONSU (1996). A 90^0 segment of a confined aquifer was simulated, which was contained in a tank made of 2-mm thick steel plate. A 100 mm nominal diameter stainless steel well screen (0.50 mm slot size) was placed at the apex of the physical model. The segment had a radius of 1.30 m and 0.50 m thick (Figure 5.6.). The upper and lower boundaries were impervious, while the outer boundary head was constrained by contact with a reservoir and a drainage pipe. The infiltration rate was kept constant by a controlling flow device. Arrangements were made at the wellhead to use compressed air for pumping from the recharge well, enabling the redevelopment of the well. Confined conditions were preserved by means of a bolted rubber gasket placed on top of the segment.

Three series of experiments were conducted (Table 5.5.). The differences among the series consisted in: [1] the grain size distribution of both the suspended particles in the injection water and the aquifer sand grains (Figure 5.7.), [2] recharge rates and [3] the presence or absence of a gravel-pack. Aquifer transmissivity remained at 10 m^2/d for the three series. Just the concentration of injected solids changed within each series, while the rest of variables remained fixed.

Table 5.5. Summary of the experimental runs for case KWAD (OSEI-BONSU, 1996).
The transmissivity of the aquifer (10 $m^2 \cdot d^{-1}$) was never affected in the three series experiments. Clogging in the A-series (without gravel-pack) restricted to the well face. In contrast, initial transmissivity of the gravel-pack decreased from 224 $m^2 \cdot d^{-1}$ in run B1 down to a final value of 8 $m^2 \cdot d^{-1}$ in run C9. The initial transmissivity of the gravel-pack for each run is denoted by T_0, whilst the final value after recharge is expressed by T_f (B and C-series).

A-SERIES (Q=2 l·min^{-1})				**B- & C-SERIES (Q=10 l·min^{-1})**						
RU	TI	[TS	part	RU	TI	[TS	part	gra	T_0	T_f
A1	72	10	a	B1	14	10	b	B	224	29
A2	27	10	a	B2	12	20	b	B	274	24
A3	14	10	a	B3	13	40	b	B	146	7
A4	20	5	a	B4	13	20	b	B	109	11
A5	51	30	a	B5	7	10	b	B	60	28
A6	50	40	a	B6	14	20	b	B	57	9
A7	36	5	a	B7	12	10	b	B	23	6
A8	25	60	a	B8	12	10	b	B	71	9
A9	26	5	a	B9	13	40	b	B	37	7
A1	30	20	a	B1	13	40	b	B	25	7
A1	27	20	a	C1	12	10	c	C	41	7
A1	31	30	a	C2	12	20	c	C	10	3
A1	36	20	a	C3	13	45	c	C	13	5
A1	24	40	a	C4	12	10	c	C	9	4
A1	37	10	a	C5	13	20	c	C	7	3
A1	32	10	a	C6	12	45	c	C	6	3
A1	36	5	a	C7	12	60	c	C	6	3
				C8	12	30	c	C	6	3
				C9	12	15	c	C	8	6

*The notation in the columns 'part. type' and 'gravel-pack' is also used in Figure 5.7., where the grain size distribution of the injected suspended solids is indicated with lowercase letters.

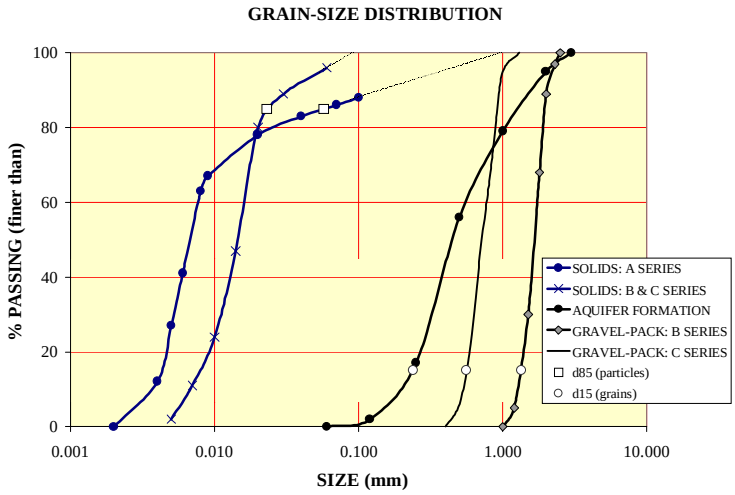

Figure 5.7. Grain size distribution of suspended particles, aquifer and gravel-pack in the three series (case KWAD).
A runs were conducted without a gravel-pack. The grain size diameter of suspended solids was also different to the one of B- and C-series. These were pretty similar, although the grain size of the gravel-pack was larger for the B-series (preserving the shape of the curve). From OSEI-BONSU (1996).

The experiments can be grouped in:

a) Non gravel-packed experiments (A-series). The runs were conducted at a constant injection rate of 2 $L \cdot min^{-1}$ in the absence of a gravel-pack, leading to a reversible blocking of the bore face. The reproducibility of these experiments was poor, because there were significant variations in the magnitude and even in the shape of the piezometric response among runs with identical starting conditions (Figure 5.8.).

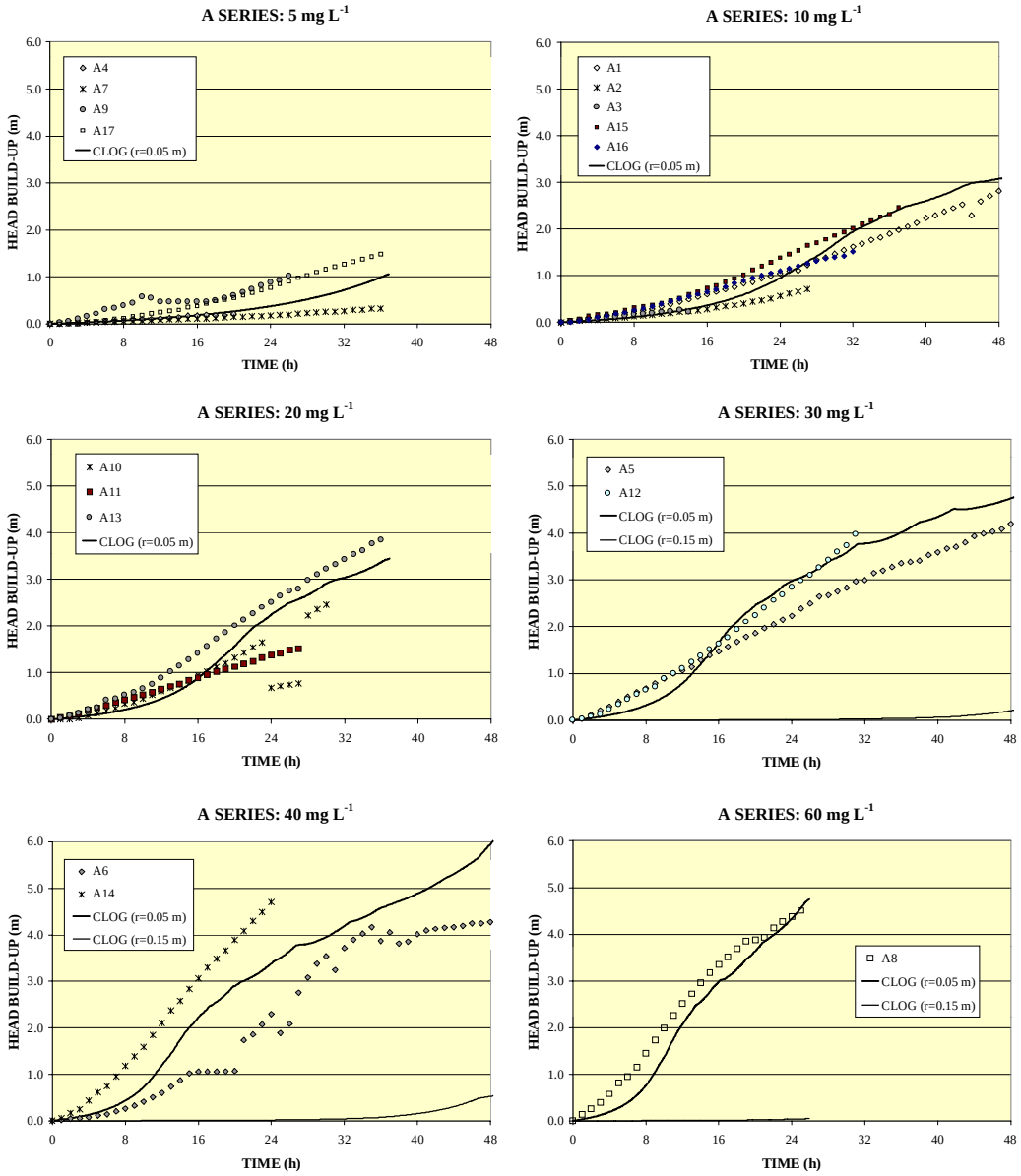

Figure 5.8. Piezometric head for the different runs of KWAD example as computed by the model. A-series: Evolution of the clogging build-up (referenced to the steady state with no suspended particles in recharge water) with respect to the concentration of suspended solids. Computed heads with CLOG are indicated with a solid line. Modified from OSEI-BONSU (1996).

b) Gravel-packed experiments (series B and C). A gravel-pack was placed between the well screen and 0.30 m radial distance, resulting in deep bed filtration. Both series operated at a recharge rate of 10 $L \cdot min^{-1}$. The only difference between the B- and C-series resided in the grain size diameter of the gravel-pack (Figure 5.7.). Because of the coarse size of the gravel-pack grains, deep bed filtration rather than blocking filtration took occurred. In B-series, clogging mainly occurred at

the interface between the gravel-pack and the aquifer sand, whilst it restricted to the gravel-pack for the C-series. It was impossible to restore the initial hydraulic conditions by air-lifting, although the clogging rate was slower than for the blocking filtration situation. Although the transmissivity of the aquifer sand was always 10 m^2/d, the transmissivity of the gravel-pack sand diminished after each run (Table 5.5.) in spite of redevelopment.

OSEI-BONSU (1996) made some remarks concerning the experimental results that must be reproduced by the model. First, clogging increases with the injection rate. This is in contrast with some results from column and core experiments in the petroleum industry (TODD ET AL., 1990; VAN OORT ET AL., 1993), even though other studies have found that head loss increases with the flowrate in columns. TARE (1986) and MORAN ET AL. (1993) showed that the damage depth within porous media is also proportional to flowrate. This discrepancy can be explained by the dominant attachment mechanisms, which depend on the particular conditions of the experiment (particle and grain size diameter, concentration of solids, flow velocity, detachment and remobilization of particles).

The second finding of OSEI-BONSU was that the lower the concentration the higher the clogging build-up, for a given mass of injected particles. This could be justified by a different deposition pattern, although the physical mechanism by which the deposition geometry is affected by the concentration is not understood. Third, the lower the initial transmissivity (of the gravel-pack, in this case) the higher the head build-up.

5.3.3. MODELLING *KWAD*

A-series experiments (17 runs) were classified as a function of the concentration of suspended solids in recharge water. From this point of view, there were six cases that had to be modelled. From the data compiled in Table 5.5., it is noticeable that only four runs within C-series were comparable (C5, C6, C7 and C8), because the initial transmissivity in the gravel-pack was practically identical. This is not applicable to B-series, but series B1 and B2 were interpreted numerically to study the behaviour of the model for different clogging patterns.

All the A-series runs were subjected to surface clogging. The calibration was performed by minimising the root mean sum of squares of errors. Interpretation of series B and C, where a gravel-pack was present, was more complicated. This is due to the uncertainties caused by the redevelopment of the gravel-pack (the first piezometer within the aquifer formation was never affected, according to OSEI-BONSU). Contrarily to the A-series experiments, gravel-packed runs suffered from irreversible clogging, as evidenced by the initial transmissivity of each run (Table 5.5.) after the unsuccessful redevelopment stage. Flow reversals through compressed air presumably promoted accumulations of fines in the close vicinity of the bore face, thus altering the permeability of the sandy formation. In order to be able to compare among those runs, the following interpretations were done:

1. Runs B1 and B2, where the filter material was recently packed and it can be assumed that the transmissivity was as close to homogeneity as possible.
2. Runs C5, C6, C7 and C8, where the gravel-pack transmissivity is approximately the same (~ 6 $m^2 \cdot d^{-1}$), so that only the only changing variable is the input concentration of suspended sediments (between 20 and 60 $mg \cdot L^{-1}$).

Table 5.6. Model kinetic parameters for the radial sector (KWAD).
Model parameters obtained after calibration of each series are shown in this table. It is remarkable that the same values were applicable to all runs of the calibrated series, except for the compressibility of the particles, which varied with the input concentration of suspended solids. This very parameter was also different for B-series in comparison with the remaining two series. Such differences are attributed to the deficient redevelopment of the pack-aquifer interface and the simplifications of the model.

PARAMETER	SYMBOL	A-SERIES						B-SERIES						C-SERIES					
		Concentration ($mg \cdot L^{-1}$)						Concentration ($mg \cdot L^{-1}$)						Concentration ($mg \cdot L^{-1}$)					
		5	10	20	30	40	60	5	10	20	30	40	60	5	10	20	30	40	60
Attachment constant	λ'_{att} [$m \cdot s^{-1}$] $* 10^{-5}$	50.0						50.0						50.0					
Detachment constant	λ'_{det} [s^{-1}] $*10^{-5}$	6.0						6.0						6.0					
Critical porosity ratio	ϕ/ϕ_{crit} [-]	0.70						0.70						0.70					
Compressibility of solids	β_s [-]	25	19	15	11.5	10	8.5							25	19	15	11.5	10	8.5
Interception exponent	m_{int} [-]	1.0						1.0						1.0					

5.3.4. *KWAD* RESULTS

5.3.4.1. *A-series*

CLOG results are very satisfactory in terms of head build-up (Figure 5.8.). More important, a unique set of model parameters was used, except for the apparent clogging factor (Table 5.6.). This parameter had to be increased in order to account for clogging at lower concentrations (Figure 5.9.), which is in agreement with the observation that lower concentrations yield higher clogging rates for the same injected mass (Figure 5.10.).

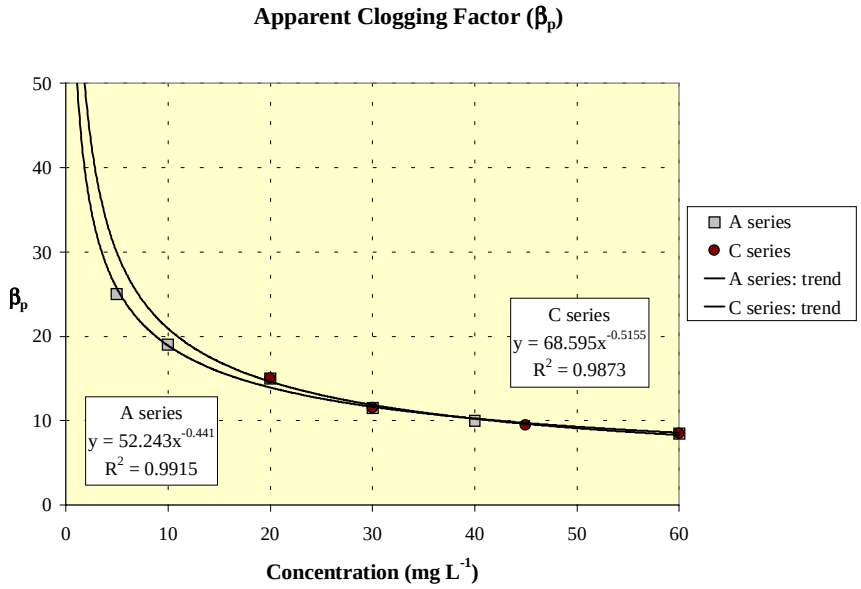

Figure 5.9. Variation of the apparent clogging factor (β_p) with concentration for the A- and C-series.
In order to reproduce the observed behaviour it was necessary to increase β_p for the lower concentrations, in accordance with the physical observation made by OSEI-BONSU (1996).

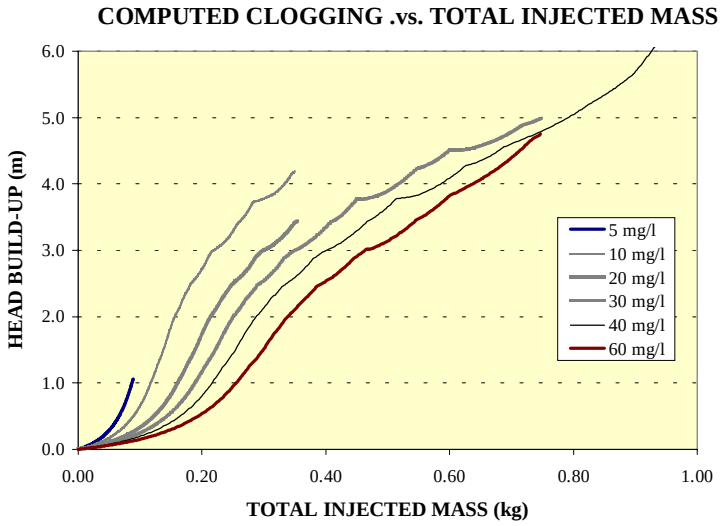

Figure 5.10. Computed clogging rate as a function of the total injected mass, for different concentrations of solids, corresponding to the A-series.
The higher the concentration, the lower the clogging rate, as observed by OSEI-BONSU. The calculations indicate that his effect is noticeable for small values of total injected mass, but it tends to be unimportant when the injected mass augments. The same can be concluded from a detailed examination of the measured data, not shown here.

5.3.4.2. *B-series*

The calibrated parameters differ from the A-series, especially as concerns the apparent clogging factor, β_s. This parameter, in accordance with the previous results, was the only one changing between runs B1 and B2 (Table 5.6.). Clogging mostly took place at the interface between the gravel-pack and the aquifer, but the model was not able to reproduce this aspect perfectly (Figure 5.11.).

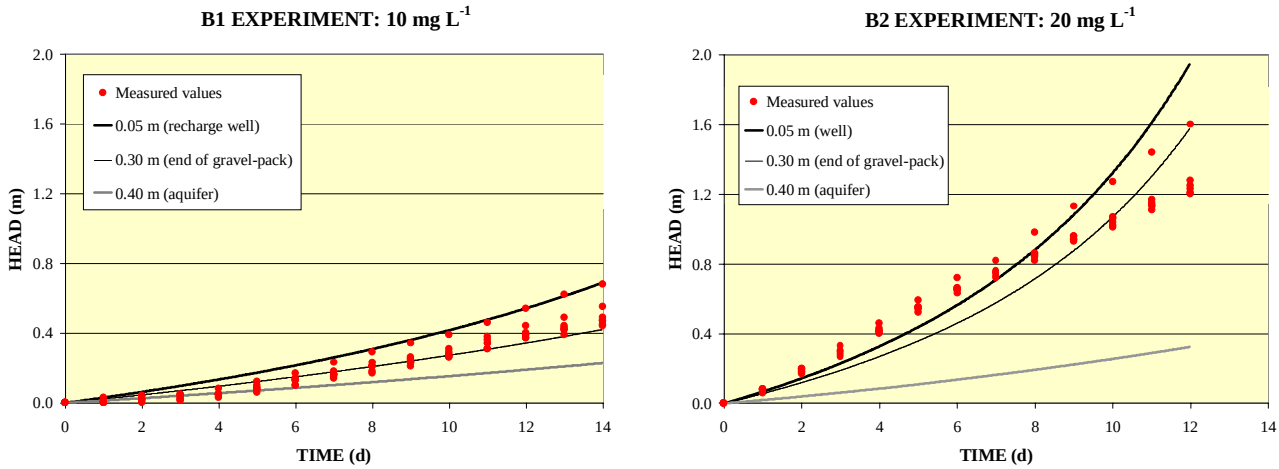

Figure 5.11. Calibration of the B1 and B2 tests with CLOG, indicated by lines for each piezometer.
The curves that correspond to piezometers located at 0.05 m (well), 0.30 m (end of gravel-pack) and 0.40 m (aquifer) are plotted.

5.3.4.3. *C-series*

All the model parameters were identical to the configuration used in the A-series (Table 5.6.), which confirms the robustness of the model. The evolution of piezometric head was conveniently reproduced by the model (Figure 5.12.) It is not surprising that the clogging rate was inversely related to the concentration of suspended particles, for a given injected mass, because the apparent clogging factor (β_s).varied like in A-series (Figure 5.9.).

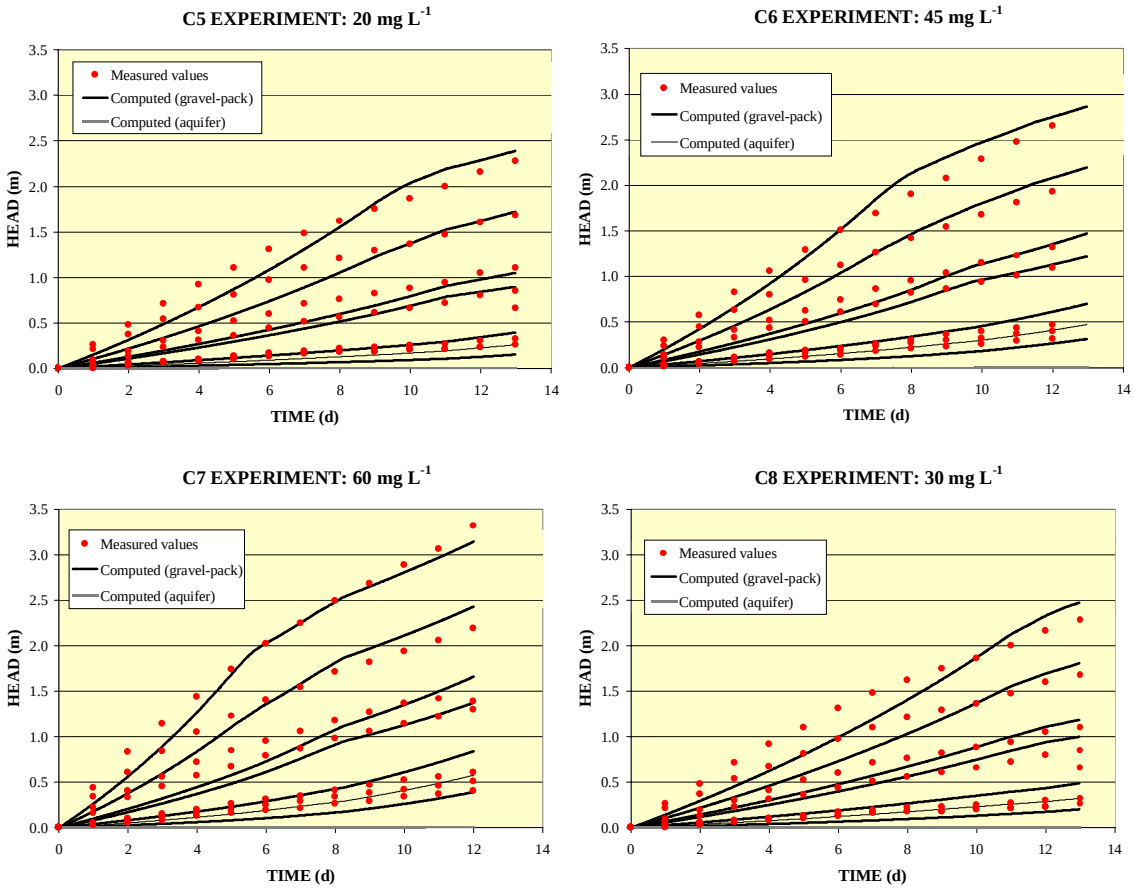

Figure 5.12. Calibration of comparable C-series experiments (C5 to C8).

5.3.4.4. *Influence of initial transmissivity*

Figure 5.13. shows the effect of initial transmissivity on head build-up for run C5. This plot compares the measured and calibrated response (for a value of 5 $m^2 \cdot d^{-1}$) with two hypothetical situations (initial transmissivity equal to 1 and 10 $m^2 \cdot d^{-1}$).

In accordance with the measured response, head build-up increases with decreasing initial transmissivity. Also, the ratio of final to initial transmissivity is lower the higher the initial transmissivity, indicating that the relative reduction is comparatively more intense.

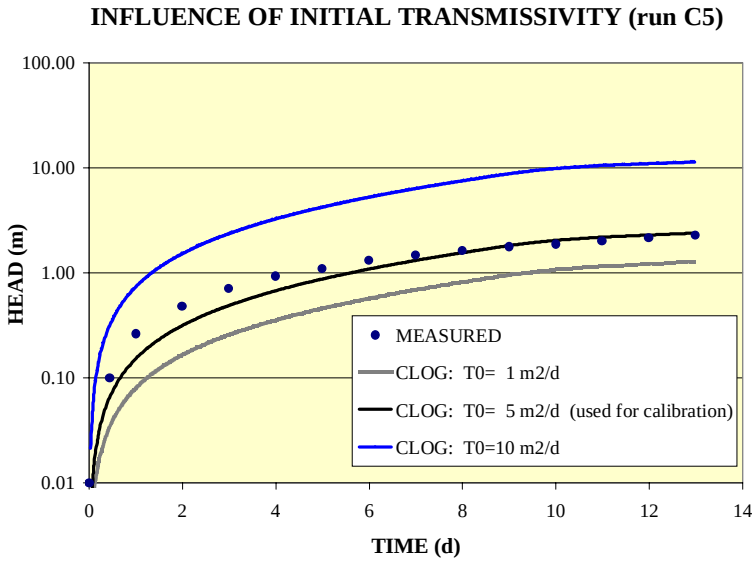

Figure 5.13. Effect of the initial transmissivity.
Measured heads are compared with the calibrated values for the adequate transmissivity of the gravel-pack (5 $m^2 \cdot d^{-1}$) and with a hypothetical lower (1 $m^2 \cdot d^{-1}$) and higher (10 $m^2 \cdot d^{-1}$) value.

5.3.4.5. *Sensitivity Analysis*

The influence of the model parameters on the simulated results was investigated by modifying each parameter while the rest remained fixed. The specific model parameters include the attachment constant (λ'_{att}), the detachment constant (λ'_{det}), the critical porosity value (ϕ/ϕ_{crit}) and the apparent clogging factor (β_s).

With the aim of assessing the importance of other variables, the analysis included the initial porosity (ϕ_0) and the interception exponent (m_{int}). The former is usually characterised by laboratory or field determinations, whilst the latter ranges between 0.5 to 2.0 (a value of 1.0 is taken by default). This is why the uncertainty associated with these two variables is considerably small as compared to the kinetic model parameters.

Figure 5.14. presents a summary of the most influential parameters: the apparent clogging factor and the critical porosity value. Both the initial porosity and the interception exponent are also very important, but the uncertainties are considerably reduced.

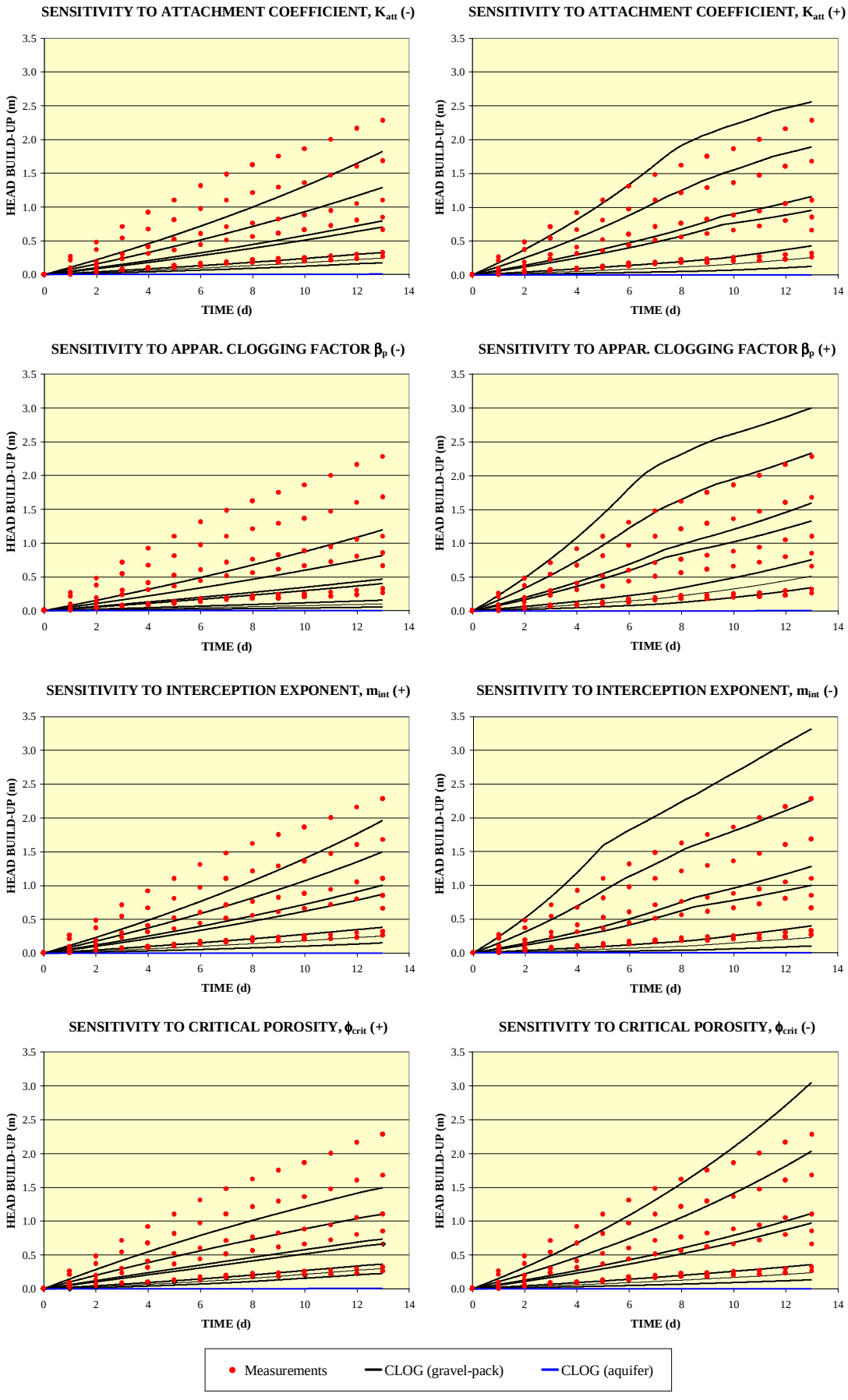

Figure 5.14. Sensitivity to the indicated model parameters, run C5 (20 mg·L^{-1}).

5.4. AEROBIC BACTERIA IN SAND COLUMNS (Arresø, Denmark)

5.4.1. INTRODUCTION TO *DANE*

Moderate concentrations of organic carbon may result in clogging of artificial recharge systems due to microbial growth. In particular, microbial activity is able to alter redox conditions in sand filters, which, in turn, has implications on water quality. This problem, discussed in Chapter II, has been recognised already (HIJNEN & VAN DER KOOIJ, 1991).

In this case, clogging in sand columns that were infiltrated with lake-water was studied by means of laboratory experiments (ALBRECHTSEN ET AL., 1998; 1999). The experimental study focused on bacterial growth during clogging in order to gain insight into the influence of some parameters from a phenomenological perspective. Clogging initiated after a brief adaptive stage, and then it became very pronounced, even though it occurred mostly in the upper part of the column.

5.4.2. EXPERIMENTAL SET-UP OF *DANE*

Infiltration water was collected at the Arrænes pilot infiltration plant (Zealand, Denmark) in autumn 1997, approximately. Water came from Lake Arresø and it was not pre-treated. The experimental set-up was not designed to reproduce the exact conditions of a specific field site, but to replicate surface recharge with water containing appreciable concentrations of organic carbon. The experiment consisted of the column, recharge water kept at 5ºC and slowly stirred, a peristaltic pump and the controlling devices (Figure 5.15.).

The column consisted of a 25 cm long and 10 cm diameter sandy material. It remained always saturated due to the imposed boundary conditions. Non-filtered lake water was recharged at the upper part of the column and drained along to a tube connected to the lower part of the column. The outlet elevation was such that it remained higher than the column height, 30 cm above the bottom of the column. The porous medium consisted of quite homogeneous quartz sand (mean diameter of grains between 0 and 0.4 mm, with a uniformity coefficient $d_{60} \cdot d_{10}^{-1}=2.0$). Several manipulations were done to ensure the absence of organic matter in the column and to achieve a homogeneous initial distribution of microorganisms throughout the column.

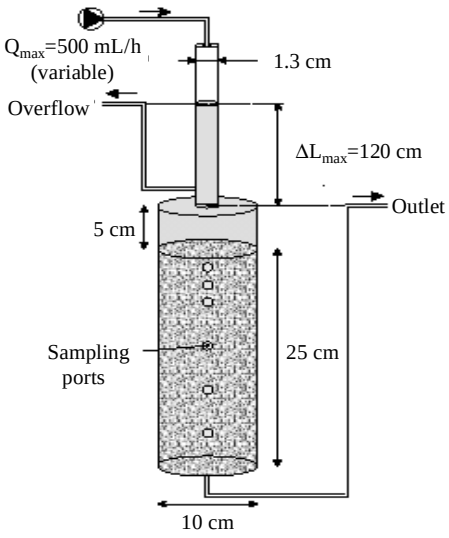

Figure 5.15. Schematic plot of DANE experiment.

The experiment proceeded at a roughly constant infiltration rate of 4.0 $cm \cdot h^{-1}$ (flowrate 400 $mL \cdot h^{-1}$), but bacterial clogging provoked an additional head build-up that increased with time. This is why a maximum pressure tube was installed, at 120 cm height. Once this level was attained the exerted pressure remained constant (120 cm) at the inlet area, thus leading to a progressive diminution of the infiltration rate. From the vertical experimental profiles it can be concluded that clogging mostly affected the upper part of the column. For instance, organic carbon accumulated in the upper 6 cm (ALBRECHTSEN ET AL., 1998).

5.4.3. MODELLING *DANE*

Given the aforementioned conditions, it was decided to simulate the first part of the response, i.e. the period corresponding to a constant infiltration rate of 4.0 $cm \cdot h^{-1}$ (24 days). This is justified because there is a relationship between head build-up and infiltration rate decrease. However, some authors postulate that certain differences could arise, because clogging mechanisms may be affected by the boundary conditions imposed to the system (BAVEYE ET AL., 1998). Maintaining the flowrate implies that some aggregates could detach from the porous medium and mitigate clogging, whilst a constant head would lead to an increasingly reduced supply of nutrients and, consequently, to a slower clogging rate.

A 1-D vertical domain was adopted since it sufficed to characterise clogging in this example. A constant infiltration rate (4.0 $cm \cdot h^{-1}$) was imposed in the upper node, whilst constant pressure (equivalent to 0.30 cm piezometric head) was applied to the lower one. Initial hydraulic permeability was $5 \cdot 10^{-5}$ $m \cdot s^{-1}$ (ALBRECHTSEN ET AL., 1998), whilst the effective porosity was set at 0.10 for the whole column.

The system always remained under aerobic conditions. For instance, the concentration of dissolved oxygen (DO) was higher than 3.9 $mg \cdot L^{-1}$ in the outlet of the column (leakage water at t=24 d, Table 5.7.). This is why the conceptual model just included aerobic bacteria oxidising organic matter (TOC, represented in the model as CH_2O). Dissolved oxygen and organic matter were taken, respectively, as the electron acceptor and donor. Initial and boundary concentrations for DO and TOC are indicated in Table 5.7.

Table 5.7. Initial and boudary conditions for oxygen and carbon.

	INITIAL WATER (constant)	RECHARGE WATER (constant)	LEAKAGE WATER (t=24 d)
DO (mg/l)	10	10	3.9
TOC (mg/l)	25	25	12.8
Comments	all nodes; t=0	1^{st} node; $\forall$ t	last node; t_{end}

Finally, it is important to notice that the following simple reaction was considered in the hydrochemical system of the numerical model:

$$CH_2O + O_2 \xrightarrow{\text{aerobic bacteria}} CO_2 + H_2O \qquad [5.1.]$$

5.4.4. *DANE* RESULTS

After calibration of the model parameters it was possible to obtain a satisfactory fit to laboratory data, as depicted in Figure 5.16. for piezometric head evolution at four different depths in the column. From this graph it is clear that clogging in the model concentrated in the upper part of the simulated column, in accordance with the measurements.

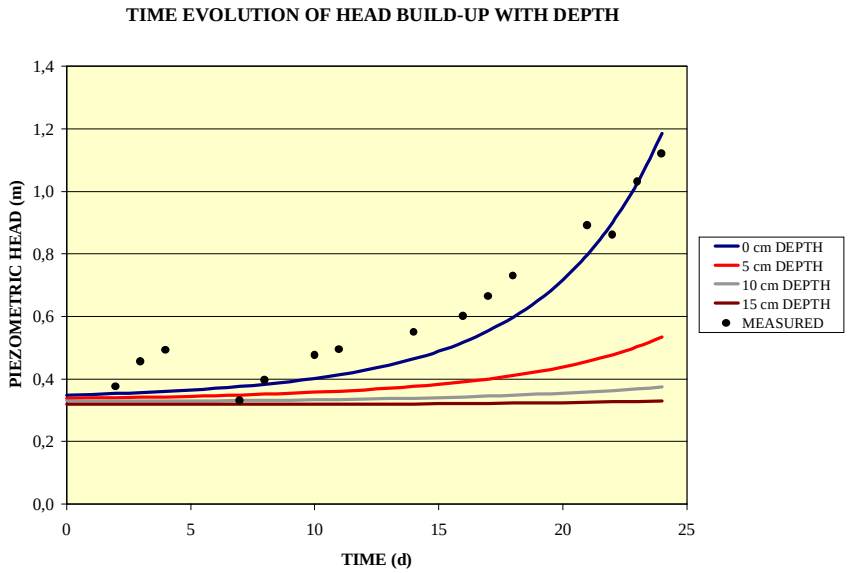

Figure 5.16. Calculated and measured heads at the inlet surface.

Figure 5.17. shows that the impact of clogging on piezometric head was only noticeable within the first 15 cm of the column. Porosity diminished throughout the whole column, although the reduction was small below 15 cm depth (Figure 5.18.). As for the quality parameters, both organic carbon and (especially) oxygen were significantly reduced, in perfect agreement with the measurements (Figure 5.19.).

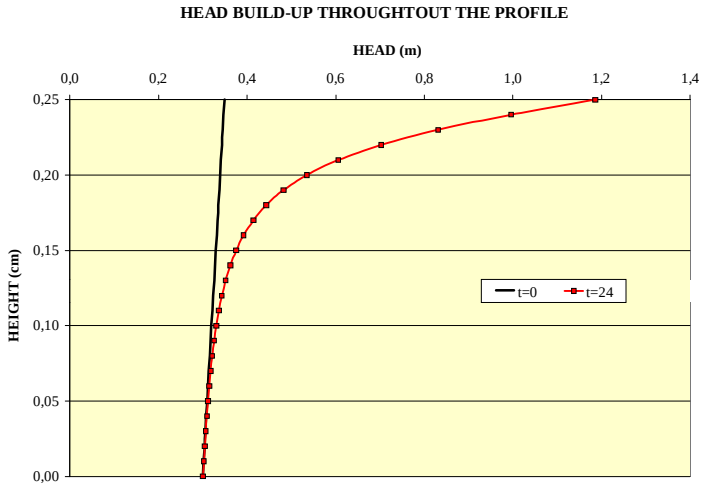

Figure 5.17. Piezometric head profile before recharge (dark line) and after 24 days infiltrating (line with squares).

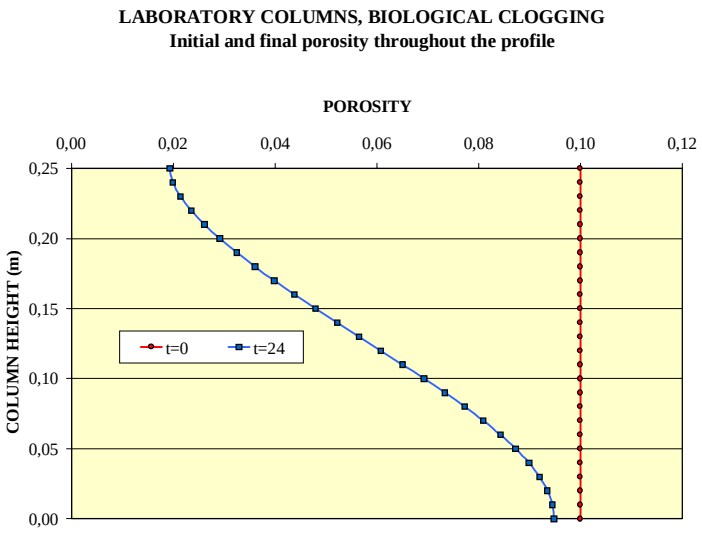

Figure 5.18. Initial and final porosity along the column.

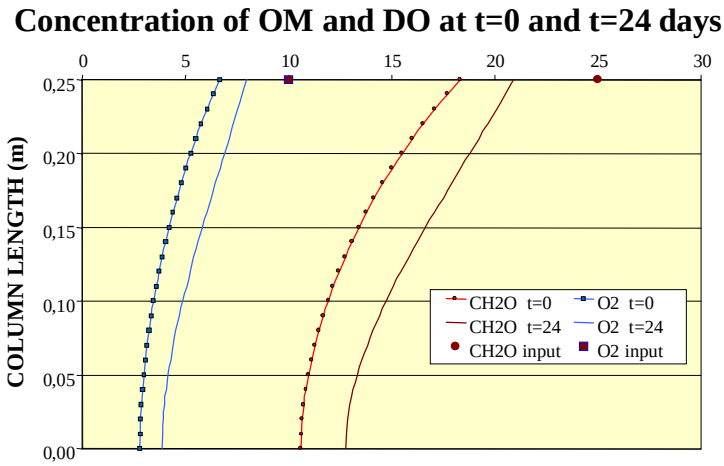

Figure 5.19. Initial and final computed concentrations of organic matter (OM) and dissolved oxygen (DO) throughout the column.

In order to obtain an indication about the plausibility of the calibrated model parameters, these were compared to values that are sufficiently known in other disciplines. Model parameters that led to the so-called 'optimum' agreement with measured data are within the range of values of the activated sludge technology (Table 5.8.). It is evident that the parameters are not comparable in quantitative terms, because of the important differences between both disciplines (for instance, activated sludge operates in open deposits, with high concentrations of organic matter and nutrients and rapid consumption of oxygen). But such comparison allows determining whether the calibrated parameters can be realistic, given that activated sludge technology is conceptually analogous to the experiment considered here.

It is also interesting to notice that clogging was fast and important even though aerobic conditions (dissolved oxygen always greater than 3.9 mg/l in the effluent, both in the experiment and the model) were naturally maintained. This observation contrasts with typical statements that clogging is mainly caused by anaerobic bacteria, although some authors point at the essential role of aerobic strains (BAVEYE ET AL. 1998).

Table 5.8. Sensitivity analysis for the bacterial growth problem.
S0 is the 'optimum' configuration; *S1,...,S10* denote modifications of *S0*. Only modified values are written; dark cells mean that the optimum parameters were used. Ranges of analogous parameters in activated sludge technology are also indicated (after METCALF & EDDY, 1991).

	$\mu_{max}*10^{-6}$ [s^{-1}]	$\mu_{dec}*10^{-8}$ [s^{-1}]	δ_{bio} [$kg \cdot m^{-3}$]	$g_{DO}*10^{-6}$ [L^0]	$g_{CH2O}*10^{-6}$ [L^0]	Y_{DO} [L^0]	Y_{CH2O} [L^0]
Activated sludges	10÷100	4÷10	-	15÷100	15÷100	-	-
S0	1.2	3.7	4.70	25.0	30.0	1.00	2.00
S1	0.9	S0	S0	S0	S0	S0	S0
S2	1.5	S0	S0	S0	S0	S0	S0
S3	S0	4.6	S0	S0	S0	S0	S0
S4	S0	2.8	S0	S0	S0	S0	S0
S5	S0	S0	5.88	S0	S0	S0	S0
S6	S0	S0	3.52	S0	S0	S0	S0
S7	S0	S0	S0	31.0	S0	S0	S0
S8	S0	S0	S0	19.0	S0	S0	S0
S9	S0	S0	S0	S0	S0	1.25	S0
S10	S0	S0	S0	S0	S0	0.75	S0

S0 in simulations S1,...,S10 indicates that the parameter used for calibration (in S0) applies.

Moreover, a sensitivity analysis was carried out in order to study the relative influence of the model parameters. Table 5.8. collects the results of several simulations that were performed by changing one parameter while maintaining the rest of the 'optimum' configuration. Each parameter was modified by a ± 25 %., i.e. increasing and decreasing each value by 25 %.

The relative influence of each parameter is shown in Figure 5.20. It can be observed that bacterial porous density and the maximum specific growth rate are the most influential parameters, although Monod half-saturation constant also plays an important role.

All the parameters must be correctly adjusted if a satisfactory simulation of the true data is desired. This is evidenced with the initial concentration of bacteria: given a fixed configuration for the rest of parameters, one order of magnitude change in this value leads to a stationary response (i.e. no clogging). A low value is not capable of generating enough biomass growth, since bacterial kinetics (temporal net growth) depends on bacterial population. On contrary, a large value tends to enhance the role of die-off (lysis), thus compensating the cellular growth. Similar reasoning could be applied to the other variables, but the objective of this exercise was to provide insight into the model behaviour rather than to perform an exhaustive analysis.

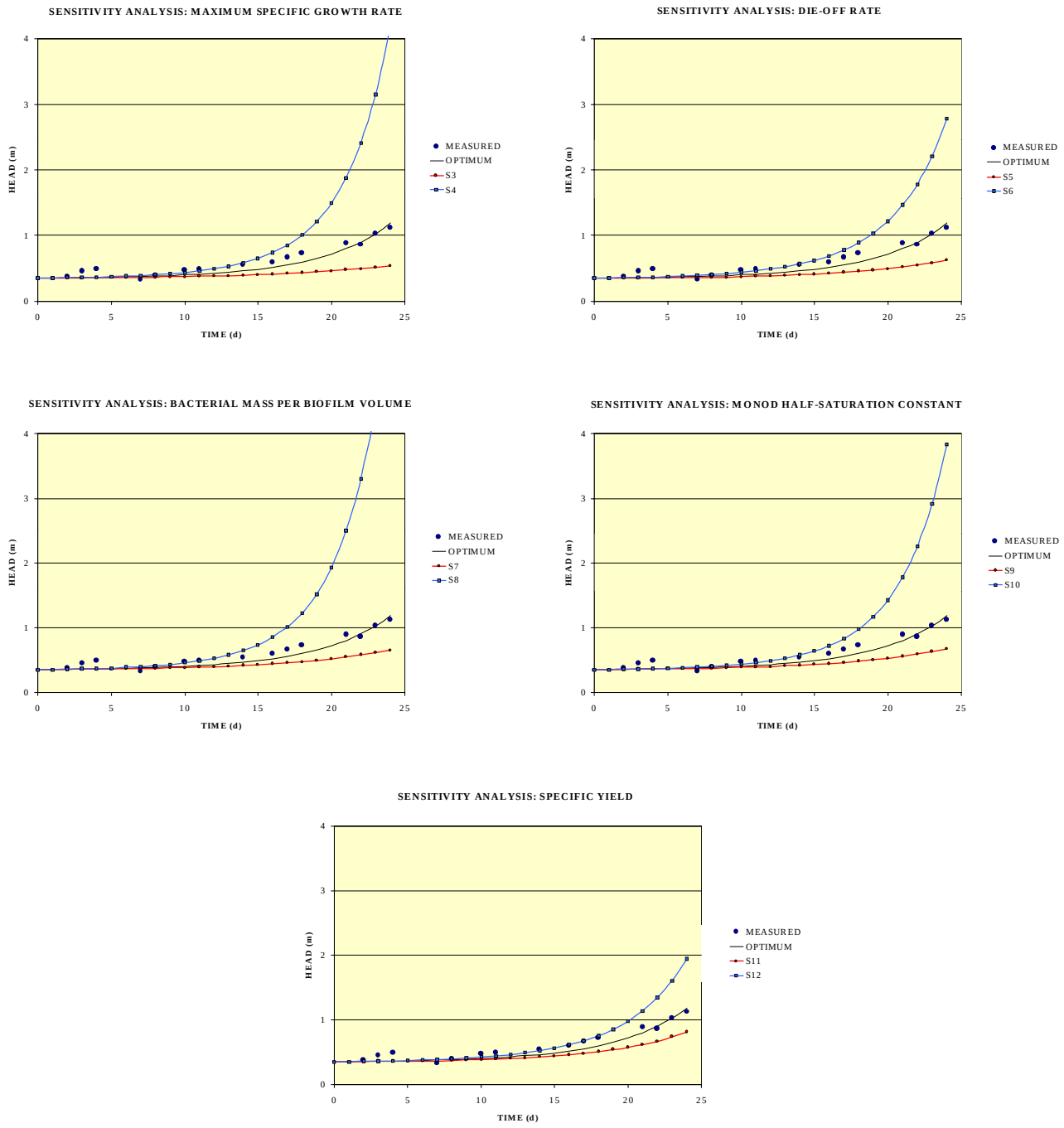

Figure 5.20. Sensitivity analysis performed with the key model parameters.

The following parameters were successively modified with respect to the optimum or calibrated value [S0]:

Up left: μ_{max} [optimum value: $1.2 \cdot *10^{-6}$ s^{-1}]. Up right: μ_{dec} [optimum value: $3.7 \cdot *10^{-8}$ s^{-1}]. Middle left: Φ_x [optimum value: 4.7 $kg \cdot m^{-3}$]. Middle right: g^{DO} -only for oxygen- [optimum value: $25 \cdot *10^{-6}$ $mg \cdot L^{-1}$]. Bottom: Y^{DO} -only for oxygen- [optimum value: 1.0].

Each simulation was run by changing one of the parameters (reduction/increment by 50 %) while the rest of parameters remained fixed.

5.5. PHYSICAL, BIOLOGICAL AND CHEMICAL CLOGGING IN CALCITE COLUMNS (Adelaide, South Australia)

5.5.1. INTRODUCTION TO *STEPH*

Artificial recharge of treated effluent is being considered as an additional means of increasing water resources in arid and semiarid areas. One of such areas is the State of South Australia, Australia, where the injection of treated wastewater is being analysed to determine the feasibility of large-scale recharge plants in the country. A 3-year project is underway in the limestone aquifer T2 of the Northern Adelaide Plains (GERGES, 1996), 30 km north from Adelaide, capital of South Australia. The aim is to store secondary effluent, which is post-treated by dissolved air flotation and filtration (DAF/F), in a sandy limestone aquifer. The final objective is to reclaim the injected water for non-potable reuse, mainly irrigation. More details on the project can be found in BOSHER ET AL.(1998).

The project will determine the technical feasibility, environmental sustainability and economic viability of ASR wells using wastewater. One of the major technical concerns was well clogging during recharge due to bacterial growth, suspended solids and gas binding. Therefore, the main water quality parameters for this kind of experiments are suspended solids (TSS) and the nutrients that will be introduced in the groundwater environment. Even though the effluent will be chlorinated to minimise bioclogging, three columns containing aquifer cores were installed to assess the biochemical compatibility of non-disinfected recharge water with the aquifer material and the native groundwater. The aim was to adopt the worse possible conditions so as to ensure the technical viability of the project (RINCK-PFEIFFER ET AL., 1998; 2000).

5.5.2. EXPERIMENTAL SET-UP OF *STEPH*

The columns were packed with cores of aquifer T2 from the Northern Adelaide Plains, corresponding to a depth of 117 metres (RINCK-PFEIFFER ET AL., 1998; 2000). The mineralogy of the core was determined by X-ray diffraction (XRD), being formed by 41 % quartz [SiO_2], 49 % calcite [$CaCO_3$], 4 % ankerite [$CaFe(CO_3)_2$] and 4 % microcline. The columns recipient was made from clear plexiglass and covered with aluminium foil to minimise the growth of photo-autotrophic organisms. They were 16 cm in length and 2.5 cm internal diameter, the pore volume being approximately 30 mL. Injection rate was constant, at 208 $mL \cdot h^{-1}$ (Darcy's velocity of 10 $m \cdot d^{-1}$), which corresponded to an average residence time of 0.14 h. The columns remained under saturation conditions during the runs.

The columns were kept at the same temperature as the target aquifer, 20°C, and were initially dosed with native groundwater to achieve a situation as close as possible to the natural conditions. Liquid pressure, flowrate and field chemical parameters -pH, temperature, redox potential, dissolved oxygen, electrical conductivity and turbidity- of both the influent and effluent wastewater were measured daily. Other chemical parameters, such as cations, anions, metals, *E.coli* and total bacterial count, were analysed every 2-3 days.

Table 5.9. presents information on the average composition of recharge water (recycled wastewater), although there were fluctuations in pH and the concentration of suspended solids. The columns were dismantled after the completion of the tests and analysed for total bacterial count, polysaccharides and calcium throughout along the vertical axis (16 cm). As for native groundwater, which was used to flush the column, available information included suspended solids (60 $mg \cdot L^{-1}$), the total Kjehldal nitrogen or NTK (0.21 $mg \cdot L^{-1}$) and phosphorous (0.04 $mg \cdot L^{-1}$).

Table 5.9. Recycled water quality containing the average quality of wastewater after DAF/F, prior to injection into the laboratory columns (from RINCK-PFEIFFER ET AL., 2000).

PARAMETER	UNITS	VALUES
Dissolved oxygen	$mg \cdot L^{-1}$ of O	7
Ammonia	$mg \cdot L^{-1}$ of N	0.2 – 0.3
Nitrate + Nitrite	$mg \cdot L^{-1}$ of N	6 – 10
Total Kjehldal Nitrogen (TKN)	$mg \cdot L^{-1}$ of N	2.5 – 3.5
Phosphorus	$mg \cdot L^{-1}$ of P	0.2 - 0.3
Iron (total)	$mg \cdot L^{-1}$ of Fe	0.01 – 0.02
Assimilable Organic Carbon	mg acetate-C equiv$\cdot L^{-1}$	0.18
Biological Oxygen Demand	$mg \cdot L^{-1}$ of O	2.0 – 3.0
Chemical Oxygen Demand	$mg \cdot L^{-1}$ of O	165 – 170
Total Organic Carbon	$mg \cdot L^{-1}$ of C	18 – 20
Dissolved Organic Carbon	$mg \cdot L^{-1}$ of C	18 – 19
E.coli	cells$\cdot 100\ mL^{-1}$	15 – 280
Total bacterial count	cells$\cdot mL^{-1}$	$10^3 – 10^4$
Suspended Solids	$mg \cdot L^{-1}$	3 - 4
Alkalinity	$mg \cdot L^{-1}$ of $CaCO_3$	140 – 150
Calcium	$mg \cdot L^{-1}$ of Ca	44.5
pH	-	7.3
EC	$\mu S \cdot m^{-1}$	2,500

As a result of the experiments, three main clogging processes were found to influence the hydraulic conductivity of the columns (RINCK-PFEIFFER ET AL., 2000):

(i) Physical clogging occurred at the start of the experiment due to filtration of suspended solids at the inlet of the columns (Figure 5.21.).
(ii) Biological clogging was predominant afterwards due to biomass accumulation and polysaccharide production. Polysaccharides and biomass were found to be present primarily at the inlet end of the column (0-3 cm), where a decrease in hydraulic conductivity was observed in the first five days of the experiment.
(iii) Chemical unclogging manifested last by means of calcite dissolution, therefore reversing previous stages of physical and biological clogging.

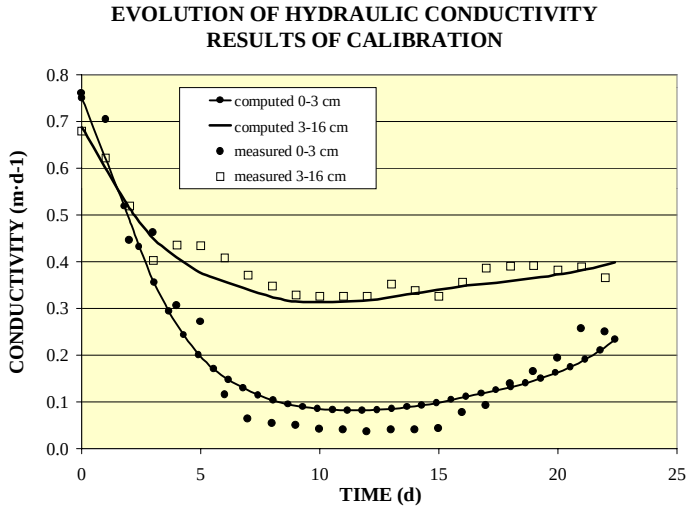

Figure 5.21. Computed and measured evolution of hydraulic conductivity in the upper and lower zones of the column. (0-3 cm and 3-16 cm).

As well as changes affecting the hydraulic conductivity, there were other significant variations as the experiment continued (Figure 5.22.). Nitrate in the outlet of the column experienced a significant increment after some days, while its concentration decreased in the second half of the run. Nitrite and ammonia were almost depleted after the passage of the effluent through the column.

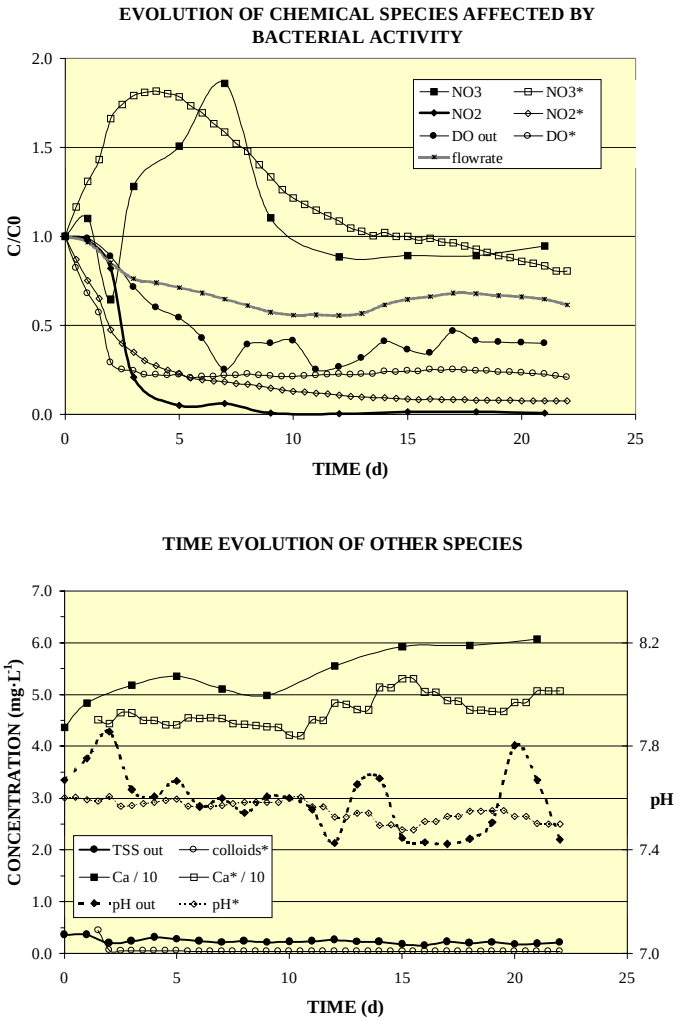

Figure 5.22. Comparison of some physicochemical parameters between measurements and numerical calibration. Lines with solid symbols refer to experimental data, whilst line with void symbols apply to computed values (indicated in the legend with an asterisk). The upper figure shows nitrate, nitrite and dissolved oxygen, normalised with respect to the input concentration (approximately constant during the whole test). Flowrate is also plotted. The lower graph shows absolute concentrations of calcium, pH and suspended solids.

5.5.3. MODELLING *STEPH*

Establishing a conceptual model is essential because the right processes have to be simulated. The starting point was to analyse the evolution of the main dissolved species to assess a plausible biochemical system. Figure 5.22. shows the evolution species that suffered a more remarkable change during recharge, i.e. dissolved oxygen, pH, suspended solids, bicarbonate, calcium, nitrate and nitrite, normalised with respect to the input concentration. Other parameters also varied noticeably, but either those changes can be attributed either to fluctuations in wastewater quality or the input concentration was not significant. Chloride exemplifies the first situation, whilst ammonium and iron are representative of the second one.

5.5.3.1. *Analysis of the data*

Several processes occurred simultaneously according to evidence shown in Figure 5.21.:

- Dissolution of calcite, as suggested by the progressive increase of calcium, bicarbonate and pH. The latter experienced many fluctuations in the input water, but still it is evident that a remarkable switch to more basic pH was registered.
- Oxidation of nitrite to nitrate. This is demonstrated by the significant reduction of nitrite, while nitrate experienced an equivalent increment between days 3 and 7. This reaction is assumed to be fast, but the composition of wastewater was presumably appropriate to promote the growth of *Nitrobacter*. Also, pH and temperature were favourable. In fact, recharge water had a constant concentration of 7 $mg \cdot L^{-1}$ oxygen in spite of the high chemical oxygen demand (170 $mg \cdot L^{-1}$). This is attributable to the post-treatment of the secondary effluent at the Bolivar plant, due to the DAF/F treatment.
- Subsequent reduction of nitrate (denitrification). After the increase originated by oxidation of nitrite, a notable continuous decrease of nitrate took place between days 7 and 12. Then, it stabilised around the input concentration. Most common denitrifiers are *Pseudomonas* spp., which help incrementing alkalinity by consuming hydrogen ions.
- Dissolved oxygen (DO) followed exactly the same pattern as nitrite, thereby confirming the nitrite oxidation hypothesis. Input of oxygen was constant during the experiment (7 $mg \cdot L^{-1}$).
- Suspended particles got retained in the column from the beginning of the experiment. The outflowing concentration was low and rather constant for the whole period. This happened irrespective of the progressive reduction of input concentration, which changed from 4 to 2.65 $mg \cdot L^{-1}$ (66 % of the initial concentration).
- Although it the behaviour of organic carbon was not conclusive (data on dissolved organic carbon, DOC, and total organic carbon, TOC, not shown), the biochemical oxygen demand was significantly reduced in the outflow end of the column. There is no data on organic matter in the core, but it could account for the relatively stable evolution of DOC. Alternatively, organic matter could be transported in colloidal form throughout the column.

5.5.3.2. *Conceptual Model*

Taking all these considerations into account, it was proposed that the numerical model included the following processes:

- Mobile species: DO, DOC, pH, calcium, bicarbonate, nitrate, nitrite and colloids. The input concentration of colloids was not constant, but it reproduced the measured evolution.
- *Generic minerals*: colloids retained in the aquifer grains, organic-carbon oxidising bacteria (denoted aerobic bacteria hereinafter), *Nitrobacter*, denitrifying bacteria and calcite. Partition between minerals and mobile species was taken to be rate-limited (kinetic reactions).
- A variable recharge rate was introduced to the model to reproduce measurements.
- Two hydraulic conductivity zones were selected, based on empirical data too. The first zone comprised the upper 3 cm of the column. The remaining of the column constituted the second zone (between 3 and 16 cm).
- The model works with liquid pressures and concentration of primary species. But measurements were processed to produce hydraulic conductivity values, so that pressures were conveniently used by the model to produce K values. Therefore, this paper will show hydraulic conductivities instead of the more classical piezometric head distributions.

The finite elements grid consisted of 32 1-D elements, 0.5 cm in length each. This includes general flow and transport parameters, total system, initial (groundwater) and recharge (wastewater) water characteristics, the explicit form of kinetic rates for the five *generic minerals*, chemical parameters and numerical parameters.

The calibration procedure was iterative and manual. The aim was to reproduce the basic trends discussed below, i.e. to obtain satisfactory results from a quantitative point of view. Therefore, an integrated calibration criterion was selected rather than focusing on the minimisation of the difference between measured and computed values for one particular variable.

5.5.4. *STEPH* RESULTS

5.5.4.1. *Results*

Figure 5.21. shows calculated and experimental hydraulic conductivity. The fit is very good, which is not surprising because it was used as the first calibration criterion. Model results reproduce all the temporal and spatial trends of conductivity in upper and lower zones of the column.

Figure 5.22. compares the computed results with the measured values of some mobile species throughout the column during the recharge period. The model reproduces reasonably well the temporal and spatial evolution of mobile species. There are acceptable differences in the magnitude of certain, but the qualitative behaviour is always consistent with the proposed conceptual model. The model tends to underestimate calcium production. This could be explained by two causes. First, the model used a time-constant input of calcium, as there were no data available. Second, denitrification consumes hydrogen ions and, consequently, rises alkalinity. The trend of pH is perfectly reproduced by the model, although the measurements reflect a more erratic behaviour, with many fluctuations. Given the buffering capacity of the aquifer matrix, it could be attributable to measurement errors.

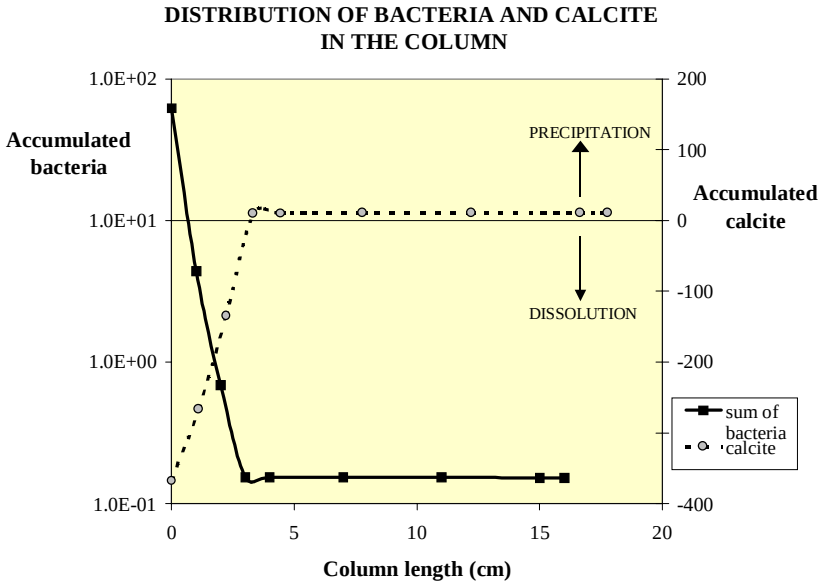

Figure 5.23. Distribution of accumulated calcite and bacteria throughout the column, as computed by the model. A strong correlation between dissolution and bacterial growth can be observed in the upper 3 cm of column. Conversely, slight calcite precipitation is associated with small bacterial populations.

Simulation of nitrogen compounds –nitrite and nitrate- is also consistent with the data. The model tends to overestimate the triggering of bacterial activity, i.e. nitrite and dissolved oxygen begin to decrease before the measurements. This is also valid for nitrate increase produced by *Nitrobacter*. The general evolution is perfectly reproduced, though. As for colloids, model results are close to the experimental results, even though CLOG (with the adopted model and parameters) does not

concede the same importance to physical clogging as seems to occur in the early stages of the experiment. Absence of data on the composition and grain size distribution of the colloidal suspension in recharge water does not contribute to clarify this point.

Figure 5.23. shows the accumulated mass of bacteria and calcite in the column, as computed by the model. The upper part of the column registered most bacterial activity, which was associated with calcite dissolution. Although not comparable in quantitative terms with experimental data, this behaviour was observed too after dismantling of the columns. The calibrated model parameters are listed in Table 5.10.

Table 5.10. Model kinetic parameters for case STEPH.

Column S0 contains the values of the parameters (optimum configuration) that led to the best agreement between computations and measurements. Simulations A1 through A6 refer to alternative scenarios that were investigated: A1 and A2 explored the effects of instantaneous dissolution and absence of calcite, respectively. A3 assumed no colloids in recharge water. A4, A5 and A6 referred to eliminating denitrifying bacteria, nitrogen bacteria and all bacteria, respectively. Simulations S1 through S6 just focused on a sensitivity analysis of kinetic parameters associated to *Nitrobacter*. Blank cells indicate that the optimum value is used, whilst grey cells highlight the change made in a particular parameter.

			Calibration	Alternative scenarios						Sensitivity analysis					
	PARAMETER	SYMBOL	S0	A1	A2	A3	A4	A5	A6	S1	S2	S3	S4	S5	S6
Physical clogging	Attachment constant	$\lambda'_{att} * 10^{-5}$ [$m \cdot s^{-1}$]	1.0			No									
	Detachment constant	$\lambda'_{det} * 10^{-7}$ [s^{-1}]	5.0			No									
	Critical porosity ratio	ϕ/ϕ_{crit} [-]	0.60			No									
	Clogging factor	Φ_s [-]	1.0			No									
	Interception exponent	m_{int} [-]	1.0			No									
Chemical clogging	Specific reactive surface	a_s [m^{-1}]	0.05		0.0										
	Kinetic reaction rate	$R^{mj} * 10^{-7}$ [s^{-1}]	4.6	∞											
	Clogging factor	Φ_m [-]	1.0												
Biological clogging	Maximum growth	$\mu_{max} * 10^{-5}$ [s^{-1}]	3.0						No						
			8.0					No	No	8.	12.				
			2.5				No	No	No						
	Die-off constant	$\mu_{dec} * 10^{-6}$ [s^{-1}]	4.0						No						
			3.0					No	No			1.5	4.5		
			4.5				No	No	No						
	Electron acceptor saturation constant	g^{ea} [$mg \cdot L^{-1}$]	3.2						No						
			3.2					No	No						
			6.2				No	No	No						
	Electron donor saturation constant	g^{ed} [$mg \cdot L^{-1}$]	15.0						No						
			4.6					No	No						
			15.0				No	No	No						
	Clogging factor	Φ_x [-]	1.0						No						
			0.5					No	No					.25	.75
			2.0				No	No	No						

It is not the objective of this section to concentrate on details of the calibration, but it is worth insisting that all the model parameters have a physical meaning and, therefore, they are constrained by physical limits. The calibrated parameters are shown in Table 5.10., together with the

modifications of this optimum configuration that were done to compare among different scenarios and to perform a simple sensitivity analysis. This is important because calibration requires much time and data, which also increases the difficulty of the system and the number of parameters involved. Validating the model with this type of experimental studies is also very important to gain insight into the range of variation of the model parameters.

Finally, it is worth remarking that the initial conceptual model was not modified during calibration. The numerical model was iteratively refined to avoid oversimplifications of reality, but the initial structure described in Chapter III was maintained.

5.5.4.2. *Alternative Scenarios*

One of the potentialities of numerical models is their flexibility to consider alternative conditions. Changing the model structure poses a limitation on the validity of new simulations and, particularly, predictive runs. The goal of this section is to compare the effect of modifying the system of minerals in order to assess the relative importance of each mineral. This is an academic analysis that does not have to be applicable to the experimental results. In particular, it is very interesting to investigate about the effect of bacteria on the performance of the recharge run, due to the concern about well clogging. As indicated above, field tests will be carried out with chlorinated recycled water, which will minimise bacterial activity.

Figure 5.24. shows six scenarios. The first one considers equilibrium dissolution of calcite, whilst the second figure is the outcome of using a negligible specific reactive surface of calcite. These are the two extreme situations as regards calcite: maximum dissolution capacity and absence of calcite dissolution, respectively. The third figure results from disregarding colloids, i.e. it represents the effect of ignoring physical clogging. Finally, the effect of bacteria is analysed: the fourth figure was obtained by removing denitrifying bacteria from the system, the fifth one without nitrogen-bacteria and the last one with no bacteria (carbon-oxidising, *Nitrobacter*, denitrifying bacteria). The last one ignores all bacteria.

It is evident that nitrogen-bacteria play a crucial role in the model, especially *Nitrobacter*. The so-called aerobic bacteria have also an effect, although its role is not as evident and its inclusion in the model might be questionable. Dissolution of calcite at the inflow end is also essential from the beginning of the experiment, whilst precipitation had also a noticeable effect on the outflow end. Suspended solids are not so influential in the conditions assumed here (low input concentration of colloids, small mean diameter of particles), but they are responsible for the early clogging stage (first two days, approximately). The simulation without bacteria (last plot in Figure 5.24.) shows that calcite dissolution is quantitative more important than colloid retention in the upper part of the column, but both processes combine to reduce the hydraulic conductivity of the remaining part of the column.

5.5.4.3. *Sensitivity Analysis*

The model has many hydraulic and transport parameters, so that it is not viable to discuss the influence of each parameter on the model results. A simple sensitivity analysis is presented in this section for the three kinetic parameters of *Nitrobacter*, i.e. the specific growth rate, decay rate and apparent density. Figure 5.25. shows that the model is very sensitive to slight variations of the kinetic parameters, which suggests that over-parameterisation is not an issue.

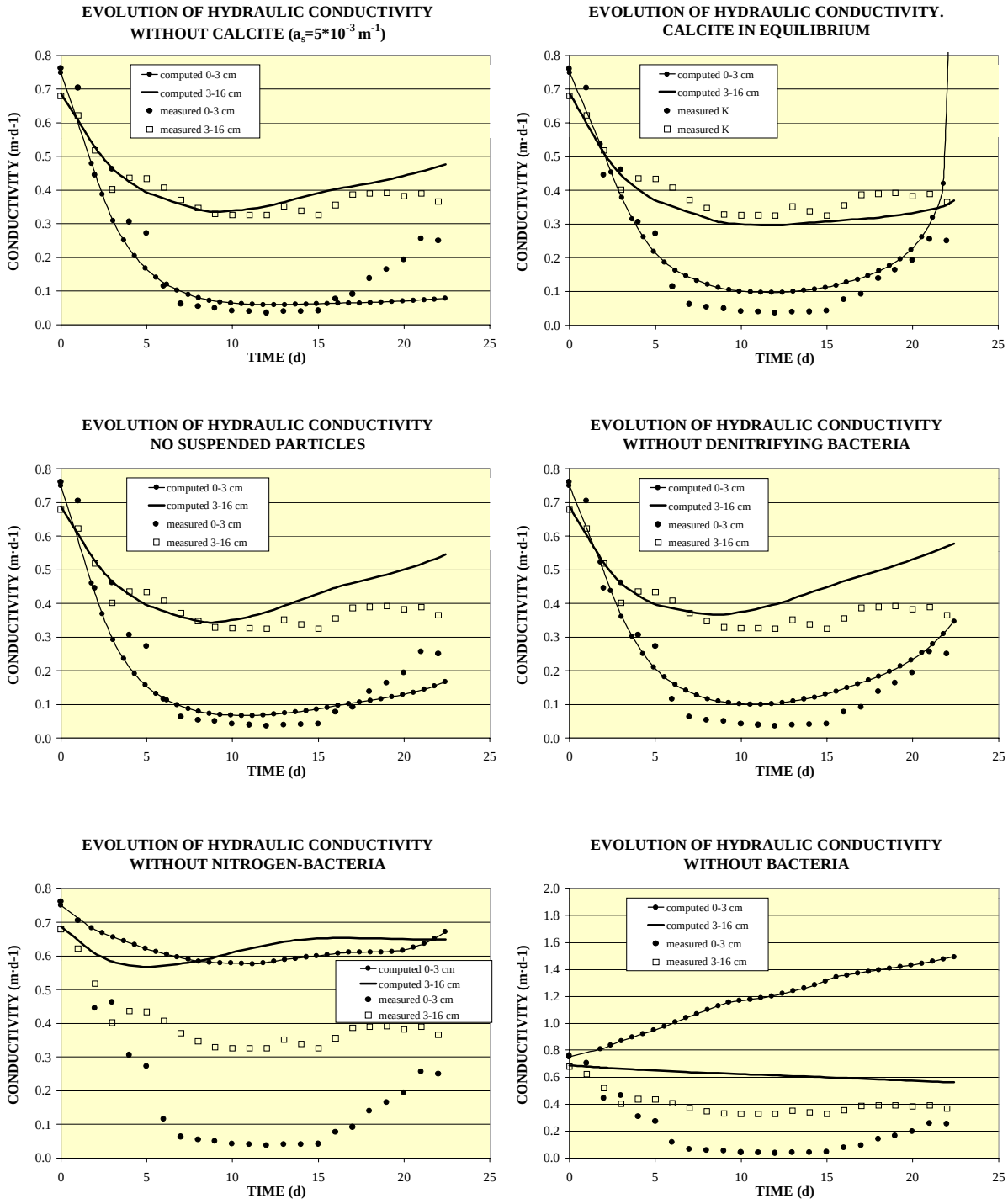

Figure 5.24. Six alternative scenarios have been investigating to assess the importance of each clogging process. They are: (1) equilibrium calcite; (2) no calcite (a_s=0.05 m^{-1}); (3) no colloids; (4) no denitrifying bacteria; (5) no nitrogen-bacteria; and (6) no bacteria. All the parameters and options used for calibration remained unchanged, except those that were meaningless due to disregarding generic minerals or mechanisms.

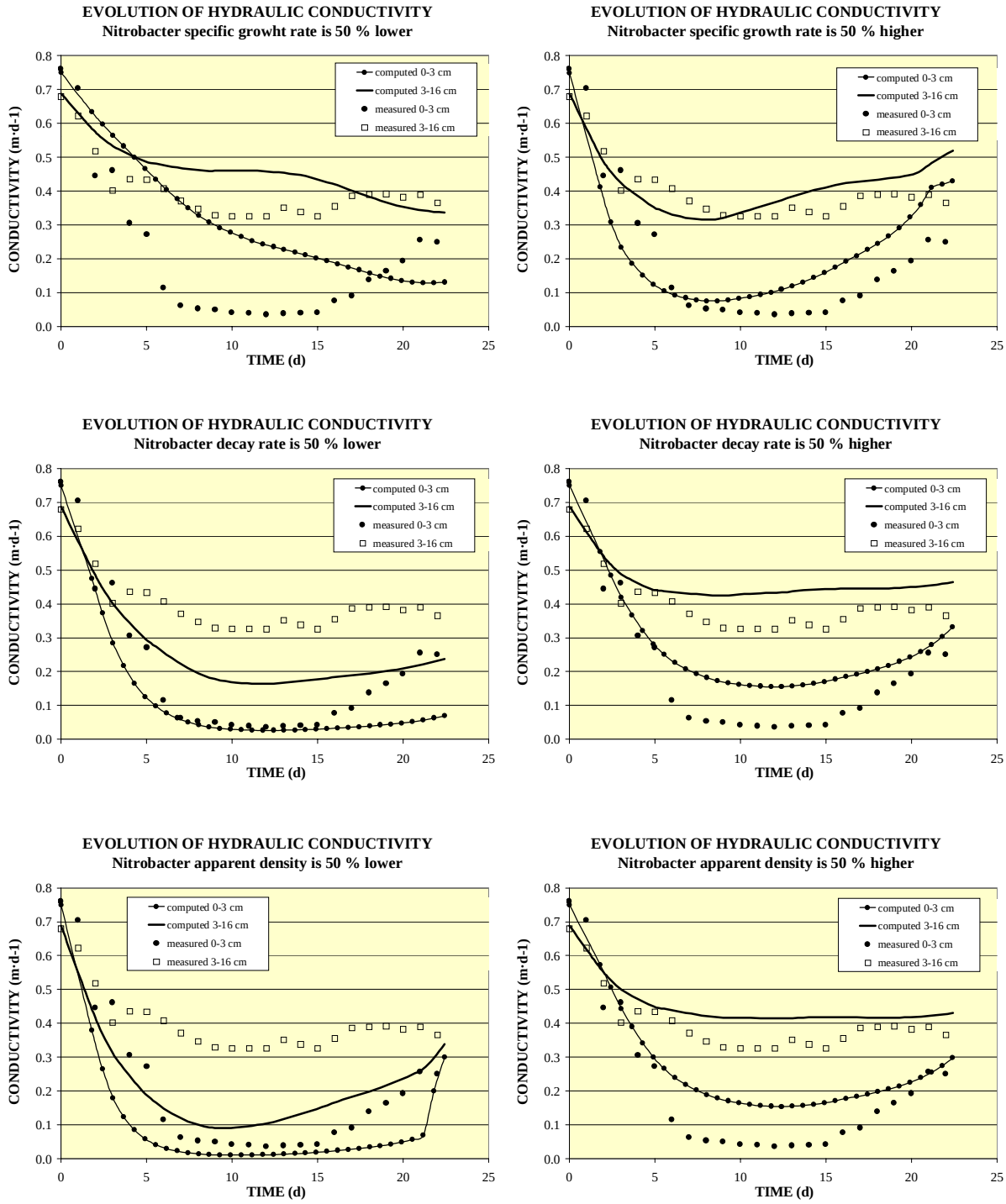

Figure 5.25. Sensitivity analysis performed with the specific growth rate, μ_{max} (above); decay rate, μ_{dec} (middle), and apparent clogging factor, Φ^{bact} (bottom) for *Nitrobacter*.
Two plots per parameter are shown, using a +50 % and a –50 % change with respect to the optimum calibrated parameter. For instance, the first plot was obtained with $\mu_{max}=12*10^{-5}$ s^{-1} and the second one with $\mu_{max}=4*10^{-5}$ s^{-1} (the optimum value was $8*10^{-5}$ s^{-1}).